Quaternary Science Reviews 251 (2021) 106659

Contents lists available at ScienceDirect

Quaternary Science Reviews

journal homepage: www.elsevier.com/locate/quascirev

New Zealand as a source of mineral dust to the atmosphere and ocean

Bess G. Koffman [a, b, *], Steven L. Goldstein [b, c], Gisela Winckler [b, c], Alejandra Borunda [b, c], Michael R. Kaplan [b], Louise Bolge [b], Yue Cai [b], Cristina Recasens [b], Tobias N.B. Koffman [b], Paul Vallelonga [d, e]

[a] Department of Geology, Colby College, Waterville, ME, USA
[b] Lamont-Doherty Earth Observatory of Columbia University, Palisades, NY, USA
[c] Department of Earth and Environmental Sciences, Columbia University, Palisades, NY, USA
[d] Physics of Ice Climate and Earth, Niels Bohr Institute, University of Copenhagen, Denmark
[e] UWA Oceans Institute, University of Western Australia, Perth, Australia

ARTICLE INFO

Article history:
Received 15 July 2020
Received in revised form
17 October 2020
Accepted 19 October 2020
Available online xxx

Keywords:
Dust and sediment provenance
Sr-Nd-Pb isotopes
Rare earth elements
New Zealand
Australia
Antarctica
South Pacific

ABSTRACT

The chemical and isotopic compositions of sediments and dust can be used to trace their provenance, providing insights into many Earth surface processes. During past glacial climates, much of the New Zealand (NZ) South Island was blanketed by erosive glacier systems that produced large volumes of sediment. We estimate the expansion of glacial outwash plains based on a sea level lowering of 130 m at the Last Glacial Maximum (LGM), and find that the Canterbury Plains in the central South Island likely expanded by 30,000 km^2, a nearly five-fold increase, while the Southland/southern Otago region may have extended southward to cover an additional ~45,000 km^2, an eight-fold increase of the coastal plain area. Considering NZ's extreme uplift and erosion rates (~10 m kyr^{-1}), the South Island, though limited in extent compared to larger Southern Hemisphere landmasses, may serve as an important dust source to the high-latitude atmosphere and ocean.

To facilitate accurate tracing of the extent of aeolian and oceanic transport of NZ dust, this study presents major/trace element and Sr-Nd-Pb isotope ratios on sediments from the major present-day dust and sediment producing regions of the South Island. The sediment compositions strongly reflect the regional geology. For example, compared to the central South Island, Nd isotope ratios in the southern South Island are more variable and show younger crustal residence ages. The combined Sr-Nd-Pb isotopic ratios show that the central NZ South Island can be distinguished geochemically from many other Southern Hemisphere dust sources. Although isotopic similarities between the central NZ South Island and more northerly regions of South America, including Central Western Argentina and the Puna-Altiplano Plateau, and Kati Thanda-Lake Eyre in Australia (based on new data in this study) hinder downstream source attribution, a key finding is that these isotopes successfully discriminate NZ from other locations in Australia, such as the Murray-Darling Basin, Northern Territory, and Western Australia, as well as southern Africa and regions of South America south of ~37°S (Patagonia and Tierra del Fuego). A comparison of the NZ data with East Antarctic ice core dust samples indicates that NZ was not a significant dust supplier to East Antarctica; rather, the East Antarctic dust compositions can be explained by dust supplied by Patagonia, Tierra del Fuego, and Central Western Argentina in South America, and West Antarctic Rift System volcanism. In contrast, the compositions of marine sediments in the Pacific sector of the Southern Ocean are compatible with mixing of South and North Island NZ dust sources, consistent with NZ's role as an active dust supplier to the Southern Ocean. New data from Kati Thanda-Lake Eyre in Australia show that it may also be a contributor, if dust from this region is able to reach the Pacific sector independent of other Australian sources.

© 2020 Elsevier Ltd. All rights reserved.

1. Introduction

Determination of detrital sediment provenance is an important

* Corresponding author. Department of Geology at Colby College, USA.
E-mail address: bess.koffman@colby.edu (B.G. Koffman).

https://doi.org/10.1016/j.quascirev.2020.106659
0277-3791/© 2020 Elsevier Ltd. All rights reserved.

tool for understanding Earth surface processes and changes in the climate system. Examples include the origins and causes of Heinrich events (e.g., Andrews and Tedesco, 1992; Hemming et al., 1998; 2000; Hemming, 2004); the influence of Saharan dust on soil formation in the Caribbean (e.g. Muhs et al., 1990); and past atmospheric circulation and climate around Antarctica (e.g. Grousset et al., 1992; Basile et al., 1997; Delmonte et al., 2004; Fischer et al., 2007). Beyond the ability to track transport patterns, knowledge of dust provenance can elucidate the influence of atmospheric deposition on marine ecosystems and, in turn, global biogeochemical cycles (e.g., Jickells et al., 2005; Moore et al., 2009). The source of atmospheric dust is closely linked to its potential influence on primary producers, whether through iron fertilization (Schroth et al., 2009; Winton et al., 2016; Shoenfelt et al., 2017, 2018) or toxic effects from metal deposition (Paytan et al., 2009).

Recent work has shown that mechanically-weathered, glaciogenic sediments contain a greater proportion of bioavailable Fe(II) than arid-region sediments (Schroth et al., 2009; Shoenfelt et al., 2017, 2019). Further, the flux of Fe(II) to the Southern Ocean increased by a factor of ~15–20 during glacial periods, implicating enhanced glacial weathering and suggesting a role for glacier-derived Fe fertilization in the observed declines in atmospheric CO_2 (Shoenfelt et al., 2018). New Zealand's South Island was covered by an erosive temperate ice cap during the Last Glacial Maximum (LGM, ~26,000–18,000 years ago), with estimated area of 40,000 km^2 (Porter, 1975; Barrell, 2011; Golledge et al., 2012). High rates of glacial erosion, coupled with some of the highest tectonic uplift rates in the world (up to 10 m kyr^{-1}; Tippett and Kamp, 1993; Hovius et al., 1997; Norris and Cooper, 2000), suggest that the NZ South Island may serve as an important source of glaciogenic Fe(II)-rich dust to the Southern Ocean.

Geochemical and mineralogical characterization of sediments in regions up-wind or up-current from deposition sites is a critical step in the process of source attribution (McLennan et al., 1993). These potential source areas *(PSAs)* serve as end-members against which to compare samples of unknown provenance. Approaches include clay mineralogy (e.g., Biscaye, 1965), Ar/Ar and K/Ar geochronology (e.g., Hemming et al., 1998, 2000, 2002), Sr, Nd, and Pb isotopes (e.g., Grousset et al., 1992, 1998; Nakai et al., 1993; Farmer et al., 2003; Grousset and Biscaye, 2005), rare earth elements (REEs; e.g., Wegner et al., 2012), and trace elements (e.g., Muhs et al., 1990; Marx et al., 2005b). The most prominent PSAs in the Southern Hemisphere are southern South America, southern Africa, Australia, New Zealand (NZ), and ice-free regions of Antarctica (Fig. 1A). While geochemical characterization of South American and Australian PSAs has been a major focus of previous studies (e.g., Delmonte et al., 2004; Gaiero et al., 2004, 2007; Gingele and De Deckker, 2005; Gaiero, 2007; Gili et al., 2016, 2017), NZ has been less well studied. Previous isotopic characterization of NZ South Island sediments includes 10 fine-grained (<5 μm diameter, most relevant for Antarctic ice-core dust studies) samples analyzed for Sr and Nd isotopes (Delmonte et al., 2004), 3 of the same samples analyzed for Pb isotopes (Vallelonga et al., 2010), and an additional 32 samples analyzed only for Nd isotopes (grain sizes not stated; Frost and Coombs, 1989). The geomorphic context and depositional age of many of these samples are uncertain.

This study aims to fill the information gap of NZ PSAs and provide a comprehensive geochemical characterization of NZ South Island fine-grained sediments representing potential dust sources. In light of the role that glaciers play as dust generators through intense physical weathering (e.g., Sugden et al., 2009; Prospero et al., 2012, Shoenfelt et al., 2018, 2019) and given recent work highlighting the importance of atmospheric transport from NZ's South Island to Antarctica (Neff and Bertler, 2015), we seek to assess the spatial variability of the South Island dust source and compare NZ sediment compositions to those of other Southern Hemisphere PSAs. To this end, we present major/trace element concentrations, including REE, and Sr-Nd-Pb isotopic ratios on more than 20 NZ sediment samples, significantly expanding existing PSA datasets. Because far-traveled dust tends to be fine-grained (e.g., 2 μm volumetric mode diameter; Steffensen, 1997), and because of potential differences in the chemical and isotopic compositions of different particle sizes, the data are measured on the <5 μm fraction. For example, in the case of Sr and Pb, the isotopic composition varies based on grain size, whereas Nd isotopes are generally indistinguishable across grain sizes (Dasch, 1969; Biscaye and Dasch, 1971; Goldstein et al., 1984; Biscaye et al., 1997; Eisenhauer et al., 1999; Smith et al., 2003; Chen et al., 2007; Gaiero, 2007; Feng et al., 2009; Meyer et al., 2011; Bayon et al., 2015), highlighting the need to compare similar grain sizes between source and sink.

This study also presents Sr-Nd-Pb isotope data on the <5 μm fraction of 14 samples from the Kati Thanda-Lake Eyre Basin (LEB) and other sites in southern Australia, previously analyzed for Pb isotopes on the bulk fraction (Vallelonga et al., 2010). We compare these data to Southern Hemisphere mid-latitude PSAs, and assess the NZ South Island as a potential source of dust to Antarctica and the Pacific sector of the Southern Ocean.

2. Background

2.1. Geologic setting of South Island, NZ: bedrock, erosion, glaciation

The NZ South Island is composed primarily of sedimentary and low-grade metamorphic rocks of Triassic to Jurassic depositional age. Argillites and graywackes of the Torlesse terrane predominate on the eastern side of the Alpine Fault (Figs. 1B, S1), grading to schist to the west and south (Mortimer and Roser, 1992; Roser and Korsch, 1999; Cox and Barrell, 2007). Neodymium crustal residence ages of these rocks typically range from 1.0 to 1.4 Ga (Frost and Coombs, 1989). Younger (Eocene to Miocene) volcanic rocks also occur on the South Island, with exposures limited to the Banks and Otago Peninsulas on the east coast, and additional smaller outcrops in southern Otago and Southland, within the Caples, Aspiring, Brooks Street, Murihiku, and Maitai terranes (Fig. S1; Frost and Coombs, 1989; GNS, 2004).

New Zealand's South Island (Fig. 1B and C) has among the highest tectonic uplift, exhumation, and erosion rates on Earth (up to 10 m kyr^{-1}; Tippett and Kamp, 1993; Hovius et al., 1997; Norris and Cooper, 2000). Within the past glacial cycle alone, an estimated 800 m of exhumation from the central Southern Alps has occurred (Herman et al., 2010), making this region a prolific source of sediment. During the last glacial period (~110,000 to ~15,000 years ago), erosion and sediment transport were primarily glacial in origin, an erosive force capable of outpacing tectonic uplift even in a tectonically active region (Gulick et al., 2015). South Island alpine glaciers expanded significantly and merged to form an ice cap with estimated area of 40,000 km^2 (Porter, 1975; Barrell, 2011; Golledge et al., 2012). For example, the largest single glacial system, the Rakaia, extended more than 60 km down-valley from its preindustrial position (Putnam et al., 2013). On the eastern side of the Alpine Fault, glacially fed streams drained onto the Canterbury Plains, a large outwash plain (Suggate, 1963). Similarly, rivers draining to the south provided sediment to outwash plains and more distal land areas above sea level in what are now the districts of Southland and Otago. Although these regions are less extensive at present, during the Last Glacial Maximum (LGM, ~26,000 to ~18,000 years ago) a sea level lowering of ~130 m (Osterberg, 2006) would have exposed significant portions of continental shelf to the

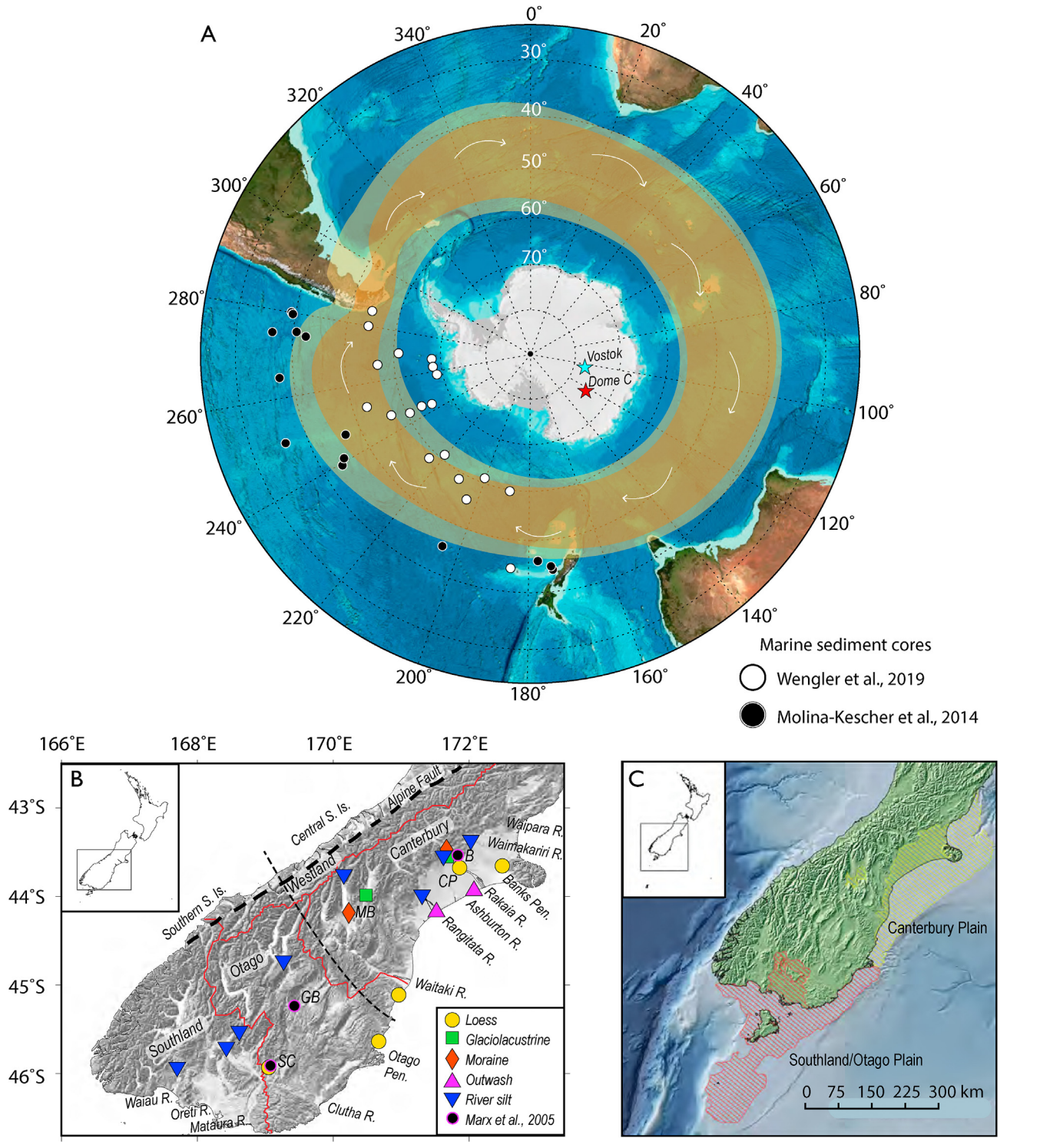

Fig. 1. A) Map showing Southern Hemisphere dust potential source areas and locations of ice and marine sediment cores discussed in paper. Yellow-orange colors show the 8 ms^{-1} and 10 ms^{-1} westerly wind contours at 850 hPa (from ECMWF ERA5 reanalysis), and white arrows indicate general wind directions. Imagery reproduced from the GEBCO Grid, version 1.3.0, www.gebco.net. B) Map of the NZ South Island showing sampling locations and types, and locations mentioned in the text (CP: Canterbury Plain; MB: Mackenzie Basin; B: Buccleuch loess; GB: Galloway Bridge loess; SC: Stewart's Claim loess). Digital elevation data courtesy of the Shuttle Radar Topography Mission (Jarvis et al., 2008). B) Inferred expansion of outwash plains and associated glaciofluvial systems based on a sea level lowering of 130 m (Osterberg, 2006; Barrell, 2011). Green shading represents land currently above sea level: yellow and red hatching indicates additional land above sea level during the LGM; these areas include mapped and inferred outwash plains, associated glaciofluvial systems, and other terrestrial landscapes above sea level that would have been exposed to the atmosphere during glacials. Red lines indicate district boundaries, as labeled on the map. (For interpretation of the references to color in this figure legend, the reader is referred to the Web version of this article.)

east and south of the South Island, significantly expanding both outwash plains and land masses in general (Fig. 1C). By comparison, to the west of the Southern Alps, glaciers terminated close to the continental shelf edge, and thus did not create areally extensive outwash plains (Barrell, 2011).

The east-west difference in glacier activity is reflected by authigenic Nd isotopic evidence from marine sediment cores indicating that the drier eastern side of the Southern Alps experienced enhanced glacial erosion compared to the wetter western side (Cogez et al., 2015). During the LGM, detrital Nd fluxes to the east were 2–8 times higher than during interglacials, while glacial/interglacial differences were negligible to the west of the South Island (Cogez et al., 2015). Thus, the areas experiencing increased erosion during glacial climates also provided sediment to extensive outwash plains, where fine-grained material would be susceptible to aeolian deflation and transport. For these reasons, our study focuses on the eastern-central and southern regions of the NZ South Island.

Glacial erosion and mobilization of sediment was significant in NZ. For example, glacial outwash and braided river sediments deposited over the past ~400 ka reach thicknesses of up to 650 m on the eastern side of the South Island (Bal, 1996). Evidence of the production and aeolian transport of fine-grained material is also widespread, with meters-thick loess deposits in places, and mass accumulation rates of ~70–150 g m^{-2} yr^{-1} on the South Island (Eden and Hammond, 2003). Indeed, loess deposits >1 m thick blanket 10% of NZ's land area (Raeside, 1964; McCraw, 1975). While modern observations demonstrate Australian dust transport into NZ (e.g., Marx et al., 2005a; McGowan et al., 2000; 2005), current evidence suggests that NZ loess deposits were sourced primarily from glacially-fed NZ river valleys (Alloway et al., 2007), a finding supported by our results. The spatial distribution of NZ dust in the Southern Hemisphere and its possible impact on Southern Ocean biogeochemistry are largely unconstrained.

2.2. Transport of dust from New Zealand

Neff and Bertler (2015) assessed the transport of dust from NZ and other midlatitude dust source regions using HYSPLIT air mass forward trajectory modeling, and found that transport of dust from NZ toward Antarctica and the Southern Ocean was favorable during all seasons. They suggested that this consistently strong transport could make up for the relatively small size of the NZ South Island, making it a significant supplier of dust to the high southern latitudes. General circulation model *(GCM)* approaches to modeling Southern Hemisphere dust transport and deposition to date have not included NZ as a potential source. However, results from these studies are consistent with the finding of Neff and Bertler (2015): both CCSM and GFDL simulations show consistent westerly and southwesterly transport from Australian dust source regions (model results by Li et al., 2008; Albani et al., 2011), which in turn can be extended to NZ. In fact, both models (neither of which included NZ as a source) show Australia as the dominant supplier of dust to the Pacific sector of the Southern Ocean.

Although the westerlies are not directly responsible for Australian dust entrainment, which is largely the result of cold fronts associated with contrasting wind and temperature gradients (De Deckker, 2020 and references therein), the average position of the westerlies does appear to influence the net transport of dust from Australia into the Tasman Sea. For example, the Tasman Sea contains a plume of deposited dust that extends eastward from the Australian continent (Hesse, 1994). As NZ's South Island lies 7–12° to the south of Australia's major dust source regions, it is more directly in the path of the Southern Hemisphere westerlies in all seasons (Fig. 2). Thus NZ fine-grained sediments may be more susceptible to wind erosion by the westerlies, and associated low pressure systems and fronts, than Australian sediments.

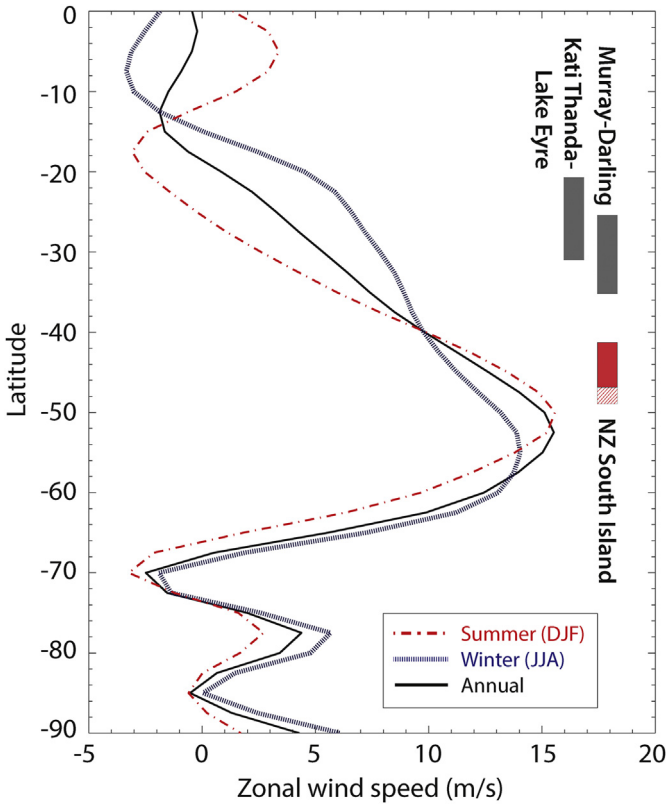

Fig. 2. Zonally averaged zonal (west-to-east) 700 mb wind speed for the Australia-New Zealand sector of the southern Indian and Pacific Oceans (i.e., 100° E to 180° E) from NOAA NCEP reanalysis, 1979–2015 (Kalnay et al., 1996). Summer (DJF) winds have a clearly defined peak at 50° S, while winter winds (JJA) are more evenly distributed by latitude. Approximate latitude ranges of major Australian and NZ South Island dust source regions are indicated by colored bars on the right. The hatched region shows the southward extension of the NZ South Island land mass during the LGM, a time when the westerlies are inferred to have shifted several degrees northward, although studies do not agree on the direction or magnitude of change (Denton et al., 2010; Kohfeld et al., 2013).

Transport of NZ dust to the high latitudes may have been even stronger during glacial climates. Some paleoclimate proxies suggest that the westerlies shifted equatorward during the LGM, likely as a result of colder temperatures and a contraction of the Hadley circulation, though there is not yet consensus about the magnitude of the shift (Kohfeld et al., 2013). The inferred northerly shift during the LGM is consistent with a northward shift in the trans-Tasman dust plume, as recorded by marine sediments (Hesse, 1994; De Deckker, 2020). A northward displacement of the wind belt would move the core of the westerlies, presently located at around 52 °S (Swart and Fyfe, 2012), closer to NZ dust source regions (Figs. 1A and 2). A shift of 3–6° would align the summer core of the westerlies with the central South Island, while a concurrent lowering of sea level would extend the South Island's land mass southward to about 48.5°S (red hatched region in Figs. 1C and 2), further enhancing potential dust source areas and thus aeolian transport.

3. Results

This study presents major element, trace element, and Sr-Nd-Pb isotope ratios on the <5 μm fraction of samples from NZ South Island PSAs, and Sr-Nd-Pb isotope ratios on the <5 μm fraction of

samples from the LEB and other sites in southern Australia, whose bulk samples were previously analyzed (Vallelonga et al., 2010). All the samples were analyzed at the Lamont-Doherty Earth Observatory of Columbia University. Methods, including GIS analysis, sample collection, and analytical methods are given in the Supplementary Material. This includes a comparison between samples dissolved via hotplate digestion using HF and HNO_3 vs. sodium peroxide sintering, because in the course of these analyses we were concerned about digestion of refractory minerals by hotplate digestion. Consistent with previous studies (Bokhari and Meisel, 2017), our results show that hotplate digestions result in an under-estimate of Zr and Hf concentrations (Analytical Methods in Supplementary Information and Fig. S6). The analytical data for the study can be found in Tables S1 and S2 and are available for download from the EarthChem data repository https://doi.org/10.26022/IEDA/111726.

3.1. Sr-Nd-Pb isotopes in central and southern NZ South Island sediments

NZ South Island sediments strongly reflect the crustal age and compositional variability of bedrock parent material. In comparison with the southern South Island, samples from the Torlesse-dominated central South Island, including the Canterbury Plains and Mackenzie Basin, form a tight cluster in Sr–Nd space, with $^{87}Sr/^{86}Sr$ = 0.7095–0.7165 and εNd = −6.5 to −4.0 (Fig. 3A, blue points). These fall within the εNd range of "Old Torlesse" sediments analyzed by Frost and Coombs (1989). Neodymium isotope measurements are presented as εNd, the fractional deviation in parts per 10,000 of the $^{143}Nd/^{144}Nd$ ratio from the "chondritic uniform reservoir" (CHUR) value of 0.512638 (Jacobsen and Wasserburg, 1980), calculated using the following equation: $\varepsilon Nd = \{[(^{143}Nd/^{144}Nd_{sample}/0.512638) - 1] * 10^4\}$. Lead isotope compositions of central South Island samples also fall within a relatively narrow range: $^{206}Pb/^{204}Pb$ = 18.75–19.04, $^{207}Pb/^{204}Pb$ = 15.65–15.68, $^{208}Pb/^{204}Pb$ = 38.68–38.93, $^{208}Pb/^{207}Pb$ = 2.470–2.485, and $^{206}Pb/^{207}Pb$ = 1.198–1.215 (Fig. 3B–D, Fig. S3, blue points). The southern South Island, including southern Otago and Southland, has more variable Sr-Nd-Pb isotopic compositions, with more positive εNd-values and lower $^{207}Pb/^{204}Pb$ and $^{87}Sr/^{86}Sr$ ratios, all indicating younger average crust formation ages, which may reflect the presence of Paleozoic volcanic complexes. Here $^{87}Sr/^{86}Sr$ = 0.7041–0.7140 and εNd = −4.0 to +5.3 (Figs. 3A, S3, white to orange points). These values reflect contributions from terranes of varying bedrock age, including the Caples, Aspiring, Brook Street, Murihiku, and Maitai terranes (Fig. S1, Frost and Coombs, 1989). While $^{206}Pb/^{204}Pb$ and $^{208}Pb/^{204}Pb$ isotope ratios in southern South Island sediments overlap substantially with the central South Island data, $^{207}Pb/^{204}Pb$ isotope ratios are consistently lower, which allows for discrimination between the two regions based on Pb isotope plots (e.g. Fig. 3C) as well as $^{87}Sr/^{86}Sr$ vs $^{207}Pb/^{204}Pb$ (Fig. 3B) and εNd vs $^{207}Pb/^{204}Pb$ (Fig. 3D). Loess samples are indistinguishable isotopically from other sediments, including modern glacial river silts, strongly supporting a NZ bedrock origin for all sample types. The isotopic data presented here are consistent with the few existing measurements on South Island fine-grained sediments (Fig. S3; Frost and Coombs, 1989; Delmonte et al., 2004; Vallelonga et al., 2010).

3.2. Major and trace element geochemistry and weathering effects

Sediment major and trace element compositions are very similar among samples, lacking the clear regional variability

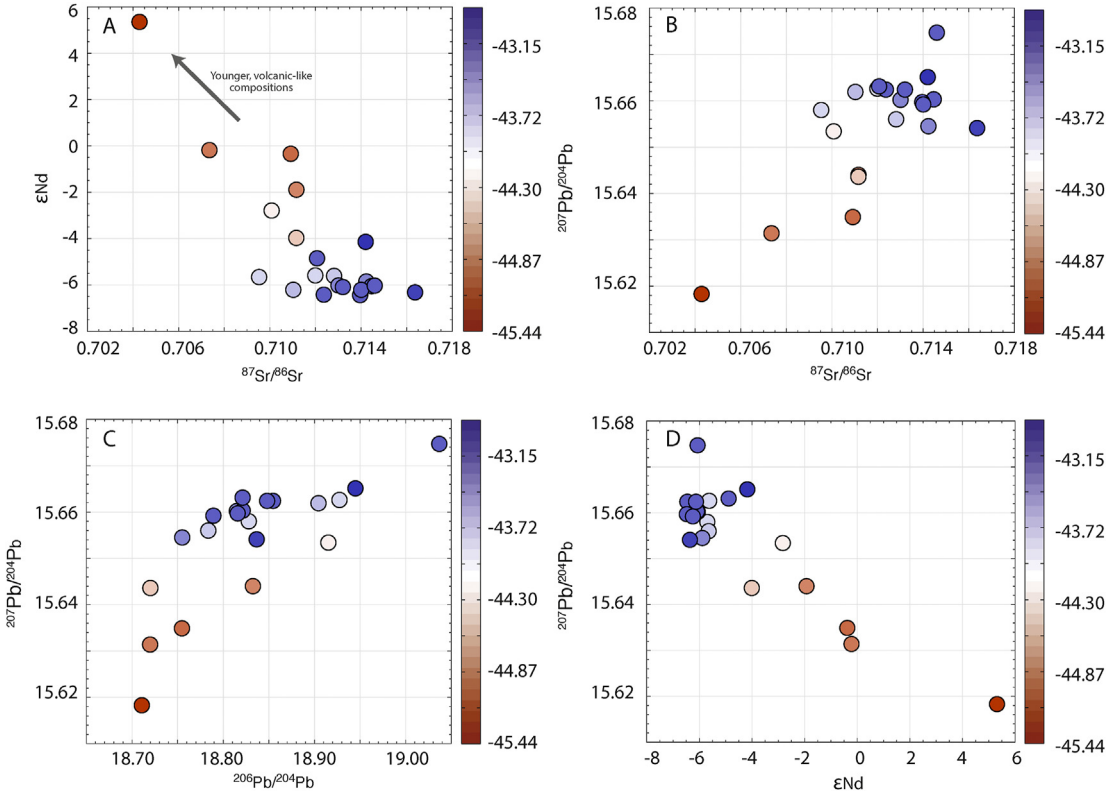

Fig. 3. Sr-Nd-Pb isotopic compositions of NZ South Island sediments as a function of latitudinal position relative to the Alpine Fault (colorbars; see map, Fig. 1B). A) εNd vs. $^{87}Sr/^{86}Sr$. B) $^{207}Pb/^{204}Pb$ vs. $^{87}Sr/^{86}Sr$. C) $^{207}Pb/^{204}Pb$ vs. $^{206}Pb/^{204}Pb$. D) $^{207}Pb/^{204}Pb$ vs. εNd. Error bars are smaller than symbols.

observed in the isotope ratios (Fig. 3). All samples have relatively flat PAAS-normalized (Nance and Taylor, 1976; Taylor and McLennan 1985; Pourmand et al., 2012) rare earth element (REE) patterns and positive Eu anomalies (Fig. S4). Our data are consistent with previously published sediment REE data, including some from the same outcrops (Fig. S4B; Frost and Coombs, 1989; Marx et al., 2005b). However, we do not observe the light REE depletion or middle REE enrichment relative to average upper continental crust (UCC) (Rudnick and Gao, 2003) described by Wegner et al. (2012).

The most prominent feature of the REE patterns is significant Ce enrichment (Fig. S4, inset). We calculate the PAAS-normalized 'Ce anomaly' *(Ce/Ce*)* as: $(Ce_{meas}/Ce_{PAAS})/[(La_{meas}/La_{PAAS})^{\wedge(2/3)} \times (Nd_{meas}/Nd_{PAAS})^{\wedge(1/3)}]$. The data show no differences in the magnitudes of Ce/Ce* as a function of latitude or region, but there are differences as a function of sediment depositional age. Modern river silts have a much smaller and less variable Ce anomaly (mean = 1.1, 1 s.d. = 0.05, n = 8) than older samples (mean = 1.54, 1 s.d. = 0.51, n = 11). In other words, longer surface residence times result in higher Ce relative to other LREE. Ages of geomorphic landforms are based on published values, and span 12–78 ka (Berger et al., 2002; Eden and Hammond, 2003; Kennedy et al., 2007; Barrell et al., 2011; Rowan et al., 2012). Previous work has shown that redox-sensitive elements are susceptible to remobilization during soil formation, with paleosols often identifiable based on negative Ce anomalies (Gallet et al., 1996). Cerium is unique among the lanthanides in its ability to have a +4 oxidation state. The large positive Ce anomalies of older samples may, therefore, indicate the formation of insoluble CeO_2 under oxic conditions, followed by the leaching and loss of more-soluble trivalent REEs. We find that among older samples, Ce enrichment is a consistent pattern across all sample types analyzed, suggesting largely oxidizing conditions since their time of deposition ~12–78 ka.

The NZ southern and central South Island samples can be discriminated based on combining trace element with isotopic data, but the distinction is almost completely based on the isotopic distinctions. While the sample population is small, we suspect that additional data will show that central South Island samples tend to have somewhat higher La/Yb and extend to lower CIA values (chemical index of alteration; Nesbitt and Young 1982), while some southern samples extend to higher Sm/Nd ratios (Figs. S5, S7). The southern vs. central data arrays also appear to confirm a shared geochemical end-member, with high La/Yb (~15), low Sm/Nd (~0.18), low εNd (~−6), high $^{207}Pb/^{204}Pb$, and high $^{87}Sr/^{86}Sr$ (Fig. S5), which is also consistent with the isotopic data variations (Fig. 3).

To assess the impact of weathering processes on measured isotopic ratios, we use the chemical index of alteration, CIA, defined as: $100*[Al_2O_3/(Al_2O_3 + CaO + K_2O + Na_2O)]$, all in wt% (Nesbitt and Young 1982). While the time scales of ~12–78 ka captured by our samples (Berger et al., 2002; Eden and Hammond, 2003; Kennedy et al., 2007; Barrell et al., 2011; Rowan et al., 2012) are too short to significantly alter the isotope ratios analyzed here by radioactive decay, some minerals are more susceptible to chemical weathering than others. For example, when fresh glaciogenic sediment is subjected to chemical weathering, minerals with high Rb/Sr and high $^{87}Sr/^{86}Sr$ ratios, such as biotite, are more easily weathered than minerals with low Rb/Sr and low $^{87}Sr/^{86}Sr$ ratios, such as plagioclase (e.g. Blum et al., 1994; Blum and Erel 1997), resulting in weathered sediment with lower $^{87}Sr/^{86}Sr$ ratios than its unweathered protolith. Thus, samples that have been exposed to weathering at the surface (e.g., moraines and outwash samples as compared with modern river silts) may have lower $^{87}Sr/^{86}Sr$ ratios along with higher CIA values. We see no systematic differences in Sr, Pb, or Nd isotope ratios as a function of CIA, sample type, or depositional age (Figs. S7, S8), indicating that chemical weathering processes operate too slowly in this environment to impact sediment isotopic compositions over the past ~80 ka.

3.3. Sr-Nd-Pb isotopes in Australian sediments

The nine new Kati Thanda-Lake Eyre Basin (LEB) sediments define relatively small fields in Sr–Nd and Pb–Pb isotope spaces (Fig. S9; Table S2). $^{87}Sr/^{86}Sr$ ratios range from 0.7093 to 0.7110 and εNd values range from −4.4 to −2.6 (Fig. 4A). These values are very similar to those previously published for this region (Revel-Rolland et al., 2006; De Deckker, 2019). Lead isotopes span relatively small ranges as well, with: $^{206}Pb/^{204}Pb$ = 18.74–19.00, $^{207}Pb/^{204}Pb$ = 15.62–15.64, $^{208}Pb/^{204}Pb$ = 38.58–38.86, $^{208}Pb/^{207}Pb$ = 2.469–2.484, and $^{206}Pb/^{207}Pb$ = 1.199–1.215 (Figs. 4B, S9; Table S2).

We also compare the LEB digested fine fraction (<5 μm) Pb isotope compositions to previously published values on the bulk fraction of the same samples, which were processed using two different approaches. Vallelonga et al. (2010) used a $HNO_3–H_2O_2$ leach for their "extracted" fraction, and a standard $HF–HNO_3–H_2O_2$ digestion for their "digested" fraction, both on bulk samples. In contrast to the interpretation that the "extracted" samples represent the fine fraction of dust (Vallelonga et al., 2010), we find that our <5 μm data match more closely with the bulk digested sample compositions (Fig. S9). Specifically, we find higher $^{206}Pb/^{207}Pb$ and $^{206}Pb/^{204}Pb$ ratios than "extracted" values, and lower $^{208}Pb/^{204}Pb$ and $^{207}Pb/^{204}Pb$ values (Fig. S9A-C). Our Pb values are more similar to that study's "digested" bulk-fraction samples, though with lower $^{207}Pb/^{204}Pb$ values (Fig. S9G). The lower $^{207}Pb/^{204}Pb$ ratios contribute to somewhat higher $^{206}Pb/^{207}Pb$ and $^{208}Pb/^{207}Pb$ ratios in the fine fraction compared to the bulk fraction (Fig. S9D-E).

We analyzed an additional five samples from southern Australia for Sr–Nd isotopes, including three from Lake Mungo and two from Brachina Gorge (locations given in Table S2). These samples have higher $^{87}Sr/^{86}Sr$ ratios than LEB sediments, with $^{87}Sr/^{86}Sr$ = 0.7144–0.7215, and lower εNd, ranging from −10.7 to −8.9, with one sample at −5.6 (Fig. 4A). We analyzed Pb isotopes on two of the Lake Mungo samples, finding: $^{206}Pb/^{204}Pb$ = 18.90–19.04, $^{207}Pb/^{204}Pb$ = 15.64–15.67, $^{208}Pb/^{204}Pb$ = 38.88–39.00, $^{208}Pb/^{207}Pb$ = 2.487–2.489, and $^{206}Pb/^{207}Pb$ = 1.209–1.216 (Fig. 4B). The Pb isotope ratios are very similar to the LEB values, though with slightly higher $^{208}Pb/^{204}Pb$ and $^{208}Pb/^{207}Pb$. In general, these values fall within the fields of other sediments from southern Australia (Revel-Rolland et al., 2006; De Deckker, 2019), with the exception of one Lake Mungo data point that has relatively high εNd = −5.6. We also observe Pb isotope offsets between our fine fraction samples and previously published "extracted" and bulk "digested" values on the same samples analyzed by Vallelonga et al. (2010), as described above (Fig. S9).

4. Discussion

4.1. Comparison of NZ to other Southern Hemisphere PSAs

4.1.1. Distinguishing New Zealand from Australia

Australia's arid environment and diverse bedrock geology lead to a large range of $^{87}Sr/^{86}Sr$ and εNd values, as represented by published PSA sediment data from the Murray-Darling Basin, LEB, Western Australia, and Northern Territory ($^{87}Sr/^{86}Sr$ = 0.708 to >0.78; εNd = −28 to 2) (Basile et al., 1997; Delmonte et al., 2004; Gingele and De Deckker, 2005; Revel-Rolland et al., 2006; De Deckker, 2019; Table S2 in this study). Given that some regions share a geologic history with NZ's South Island, it follows that the

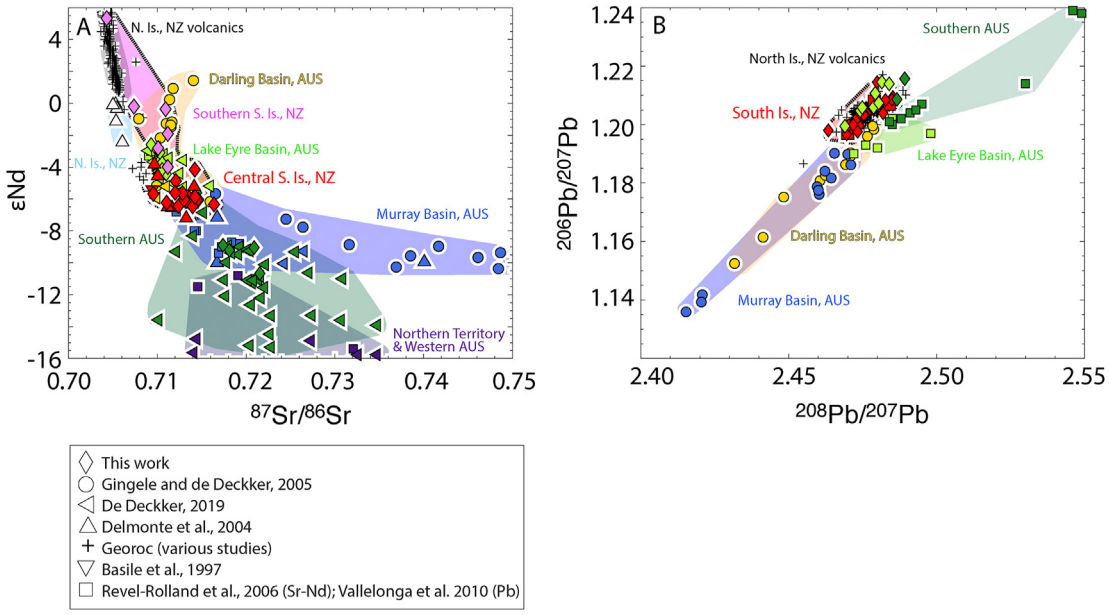

Fig. 4. Comparison of NZ and Australian (AUS) fine-grained (<5 μm) sediments. A) εNd vs. $^{87}Sr/^{86}Sr$. Note that Australian samples extend beyond the scale of the figure to the right. B) $^{206}Pb/^{207}Pb$ vs. $^{208}Pb/^{207}Pb$. Note that colors correspond by region between A and B, and not all regions in A are represented in B due to a lack of Pb isotope data on corresponding samples. There are two fields for the Lake Eyre Basin (light green) and Southern Australia (dark green) reflecting two different sample processing procedures: complete digestion of the <5 μm fraction (this study) and HNO_3–H_2O_2 extraction (Vallelonga et al., 2010); see section 3.3. Error bars are smaller than symbols. (For interpretation of the references to color in this figure legend, the reader is referred to the Web version of this article.)

isotopic compositions of some of their sediments are similar. In fact, there is substantial overlap of Sr–Nd isotopes between NZ and certain regions of South Australia and New South Wales, namely the Kati Thanda-Lake Eyre and Darling River Basins (Fig. 4A; Gingele and De Deckker, 2005; De Deckker, 2019), including the new Sr–Nd isotope data in this study. We find that LEB sediments overlap the central South Island field, though generally with slightly higher εNd values for a given Sr isotope ratio. Darling Basin sediments also trend toward higher εNd values (>−4), but do overlap the South Island field. For these locations, NZ and Australian sources cannot be distinguished by Sr–Nd isotopes. Nonetheless, there are some important dust-producing regions of Australia that can be distinguished from NZ sediments using Sr–Nd isotopes: the Northern Territory, including the Simpson Desert and area near Uluru (Ayers Rock), has εNd < −10 and $^{87}Sr/^{86}Sr$ > 0.714 (Revel-Rolland et al., 2006); Western Australia has εNd < −14 and $^{87}Sr/^{86}Sr$ > 0.714 (De Deckker, 2019); the Murray River Basin has $^{87}Sr/^{86}Sr$ > 0.716 and εNd generally < −7 (Delmonte et al., 2004; Gingele and De Deckker, 2005); and southern Australia, including Eyre Peninsula, Lake Mungo, and Brachina Gorge, has $^{87}Sr/^{86}Sr$ > 0.712 and εNd generally < −7 (De Deckker, 2019; this study). Therefore, depending on the sites of interest and on which regions of Australia were actively producing dust during the intervals of interest, Sr–Nd isotopes may be useful in discriminating sources.

Lead isotopes distinguish NZ from Australian sediments more successfully (Fig. 4B). For instance, Murray-Darling Basin sediments have lower $^{206}Pb/^{207}Pb$ and lower $^{208}Pb/^{207}Pb$ than NZ samples, while southern Australian sediments tend to have higher $^{208}Pb/^{207}Pb$ ratios (Fig. 4B). However, our new data on the fully digested fine fraction (<5 μm) of sediments from LEB overlap the NZ field in Pb isotope space. Nevertheless, for many Australian dust sources where Sr–Nd isotope ratios do not discriminate well, the combination of Sr–Nd and $^{208}Pb/^{207}Pb$ may be especially useful for distinguishing between these source regions at downstream and/or downwind sites. Unfortunately, there are limited data available with Sr-Nd-Pb isotopes measured on the same sediment samples, and the ability to determine downwind provenance would be improved if isotope ratios of all three elements were available.

Although others have documented visual and geochemical evidence of Australian dust transport to the NZ South Island (e.g., Marx et al., 2005; McGowan et al., 2000; 2005; De Deckker, 2020 and references therein), we do not see any compositional variability among NZ samples (e.g., loess vs. modern river silt from the same river valley) that would suggest a clear Australian contribution to NZ loess. It is possible that the long-term Australian contribution is swamped geochemically by a higher flux of local NZ dust.

4.1.2. *Distinguishing New Zealand from South America*

South America has variable crust formation ages, with εNd values in published PSA samples (i.e., fine-grained sediments) (Fig. 5A,B,D) ranging from −12 to +5 (e.g. Grousset et al., 1992; Smith et al., 2003; Delmonte et al., 2004; Gaiero et al., 2007; Gaiero, 2007; Gili et al., 2017). However, in contrast to the extreme range of Sr isotope ratios found in Australia, up to ~0.78 (Gingele and De Deckker 2005), South American $^{87}Sr/^{86}Sr$ values span a narrower range between 0.705 and 0.730 (Grousset et al., 1992; Smith et al., 2003; Delmonte et al., 2004; Gaiero et al., 2007; Gaiero, 2007; Gili et al., 2017). In Sr–Nd isotope space, some South American regions overlap with NZ while others are distinct. For example, the southernmost PSA regions of South America, Patagonia and Tierra del Fuego, have higher εNd (>−5) and mostly lower $^{87}Sr/^{86}Sr$ than central NZ South Island sediments, allowing separation of fields (Delmonte et al., 2004; Gili et al., 2017), although there is some overlap with the southern NZ South Island data (Fig. 5A). In Pb isotope space (Fig. 5C), the separation of NZ from Patagonia and Tierra del Fuego is distinct, and holds for both the central and southern South Island samples. On the other hand, the NZ data fields overlap with Central Western Argentina (including the Pampas), as well as the Puna-Altiplano Plateau (following the naming scheme of Gili et al., 2016), regions to the north of ~37 °S

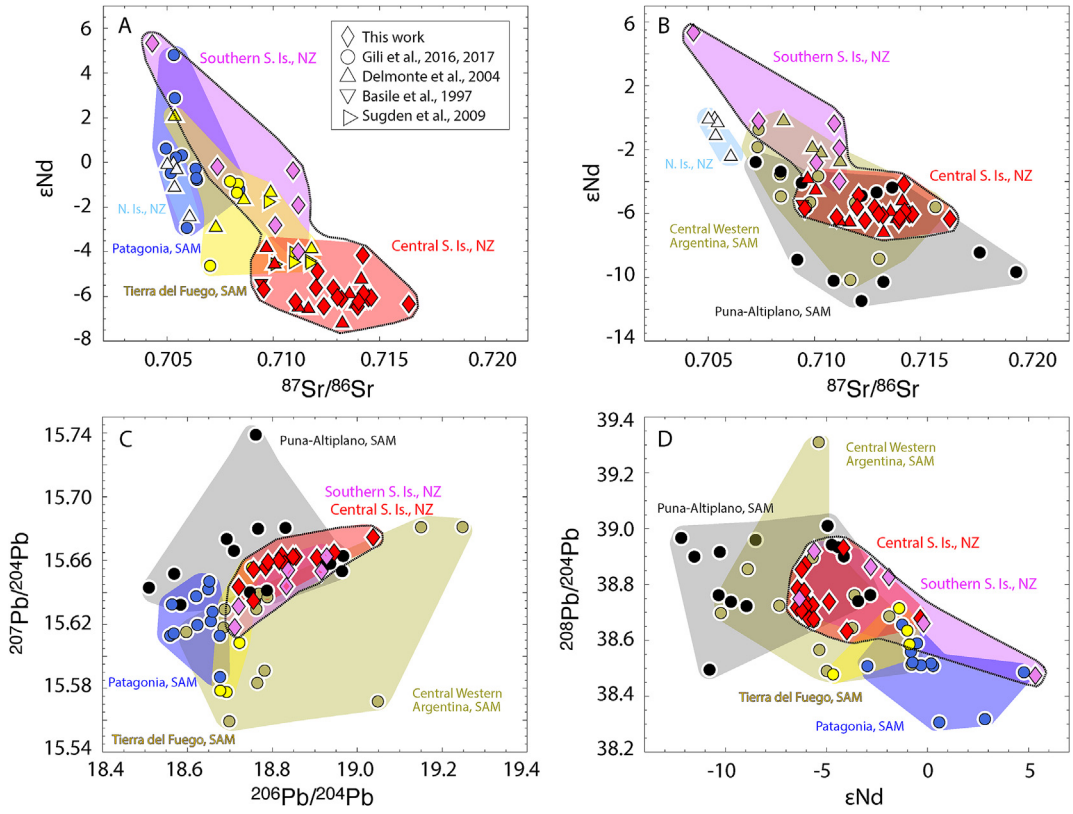

Fig. 5. Comparison of NZ and South American (SAM) fine-grained (<5 μm) sediments. A) εNd vs. $^{87}Sr/^{86}Sr$ showing that Patagonia and Tierra del Fuego have more radiogenic εNd than NZ central South Island sediments, allowing separation of fields. B) εNd vs. $^{87}Sr/^{86}Sr$ showing that Central Western Argentina and the Puna-Altiplano Plateau cannot be distinguished from NZ central South Island sediments. C) $^{207}Pb/^{204}Pb$ vs. $^{206}Pb/^{204}Pb$ showing that Patagonia and Tierra del Fuego have less radiogenic Pb isotope compositions than NZ South Island sediments. D) $^{208}Pb/^{204}Pb$ vs. εNd showing that Patagonia and Tierra del Fuego have less radiogenic $^{208}Pb/^{204}Pb$ and more radiogenic εNd than NZ sediments. Together these plots show that regions south of ~37 °S can be discriminated from NZ South Island sediments using a combined Sr-Nd-Pb approach. Naming of SAM regions follows Gili et al. (2017), with approximate latitude ranges as follows: Puna-Altiplano Plateau, 18-26° S; Central Western Argentina, 26-37° S; Patagonia, 38-52° S; Tierra del Fuego, 53-54° S. Error bars are smaller than symbols.

(Fig. 5B–D). Thus the NZ data cannot easily be distinguished from these northern South American dust source regions. Notably, these more northerly South American sources show higher geochemical heterogeneity than New Zealand's South Island as is evident from their larger ranges in the isotope plots (Fig. 5B–D). To summarize, using a combined Sr-Nd-Pb approach, the southern regions in South America south of ~37°S (e.g., Patagonia and Tierra del Fuego) can be discriminated from the key NZ central and southern South Island PSAs, in particular because they show different, non-overlapping ranges of Pb isotopes. However, the NZ sources cannot easily be distinguished from more northerly dust source regions of South America.

4.1.3. *Distinguishing New Zealand from southern Africa*

Data from southern Africa are sparse. However, the published values clearly differ from the NZ sediment signature (Fig. 6). Southern African sediments have higher $^{87}Sr/^{86}Sr$ (>0.719), lower εNd (<−8) and lower $^{208}Pb/^{207}Pb$ (<2.464) compared to NZ samples (Delmonte et al., 2004; Vallelonga et al., 2010). These regions therefore should be straightforward to distinguish from one another as end-members.

4.2. *NZ outwash plain expansion during the LGM*

Outwash plains play an important role in sediment mobilization and dust supply to the atmosphere. This is primarily for two reasons: first, glaciers produce large volumes of sediment which are effectively spread by braided streams migrating across the outwash plain; and second, glacier melt responds to temperature fluctuations on diurnal and seasonal timescales, with the net result that sediments deposited on the outwash plain routinely dry out (Sugden et al., 2009; Bullard and Austin, 2011) and provide an efficient dust source to be entrained and transported offshore.

During the LGM, NZ's outwash plains were actively aggradational (Alloway et al., 2007), and more expansive than today. Using a sea level lowering of 130 m at the LGM (Osterberg, 2006), we estimate that the Canterbury Plains likely expanded from their modern extent of ~8000 km^2 (Leckie, 2003) to cover ~38,500 km^2 (Fig. 1C). They were supplied by sediment from multiple glacially-fed braided streams, most notably the Waimakariri, Rakaia, Rangitata, and Ashburton, as well as by alluvium from non-glaciated catchments (Barrell, 2011). Farther to the south, the Mackenzie Basin, comprised of the Tekapo, Pukaki, and Ohau valleys, contained an active inland outwash plain, with water ultimately draining to the sea via the Waitaki river (Barrell, 2011). In the Southland/southern Otago region, sediment was transported primarily by the Clutha and Mataura rivers and their tributaries, including drainage from the glaciated Wakatipu valley (Barrell, 2011). We estimate an outwash plain area of ~6000 km^2 above modern sea level, based on high-resolution digital elevation data and previous work (Fig. 1; Barrell, 2011; Craw et al., 2015). During the LGM, outwash plain sediments and exposed continental shelf in Southland/southern Otago together may have encompassed 50,500 km^2, significantly extending the NZ landmass southward

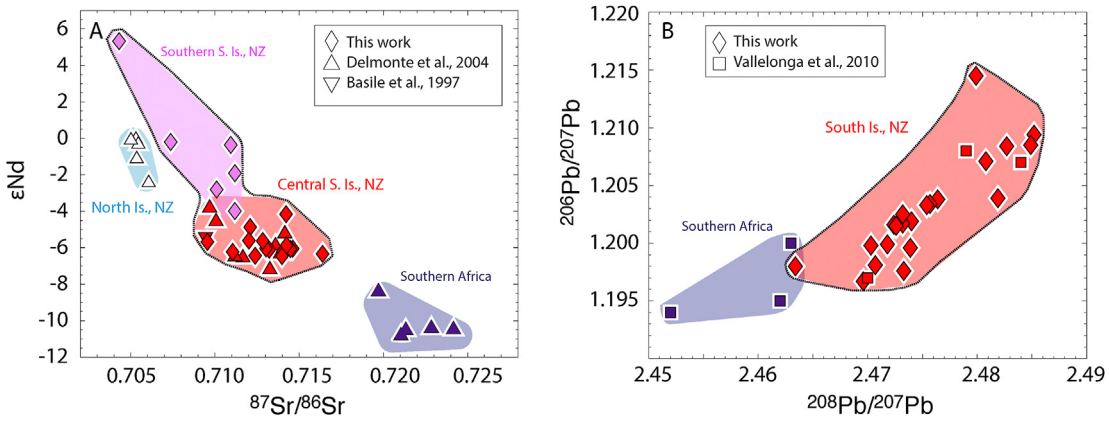

Fig. 6. Comparison of NZ and southern African fine-grained (<5 μm) sediments. A) εNd vs. $^{87}Sr/^{86}Sr$. Note that one southern African sample with εNd = −24.5 and $^{87}Sr/^{86}Sr$ = 0.7472 is not shown for reasons of scale. B) $^{206}Pb/^{207}Pb$ vs. $^{208}Pb/^{207}Pb$. Available data, shown here, suggest that Sr, Nd, and Pb isotopes are capable of distinguishing between southern African and NZ sediments. Error bars are smaller than symbols.

and into the path of the southern westerly winds (Figs. 1C and 2). Stewart Island, which has cirques and moraine-dammed ponds estimated to be of MIS 2 age, would have existed as hills surrounded by a low coastal plain (Barrell, 2011). Considering the evidence for enhanced glacial sediment production in NZ as well as the expansion of outwash plains, and exposed land area in general, we expect that during the LGM both the emissions and transport of NZ dust were likely much greater than today.

4.3. New Zealand as a source of dust to Antarctica

Much attention has focused on determining the sources of dust to Antarctica, as recorded by ice cores. The Sr-Nd-Pb compositions of dust can provide information on dust transport pathways (e.g., Aarons et al., 2016; 2017; Gili et al., 2017), changes in glacier activity (e.g., Sugden et al., 2009), and the importance of different regions in supplying iron and other micronutrients to the ocean (e.g., Winton et al., 2014, 2016). Previous studies on dust from the high-elevation East Antarctic ice cores Vostok and EPICA Dome C concluded that South America is the dominant source of dust, particularly during glacial climates (Grousset et al., 1992; Basile et al., 1997; Delmonte et al., 2004, 2007, 2010; Vallelonga et al., 2005, 2010; Gaiero, 2007, Gaiero et al., 2007; Gili et al., 2016, 2017). Most of these studies have relied on Sr–Nd isotopes, supported by modeled transport and deposition patterns (e.g., Li et al., 2008; Albani et al., 2011). However, there are significant overlaps between key dust source regions of South America, Australia, and NZ in Sr–Nd isotope space (Figs. 4 and 5), limiting the ability of these isotopes to discriminate among PSAs. In fact, one could use Sr–Nd isotope ratios to argue that NZ is a plausible end-member of dust supplied to East Antarctica (Fig. 7).

To test whether NZ was a likely source of dust to ice core sites on the East Antarctic Ice Sheet (EAIS) plateau during glacials (i.e., Vostok and Dome C ice cores; Fig. 1A), we compare the EAIS dust Nd–Sr data and Pb isotope data (none of which have Pb–Sr or Pb–Nd isotope data on the same samples) to the South American and NZ PSA data (which do have Pb-Nd-Sr isotopes on the same samples) (Fig. 8). The EAIS isotope data form arrays in Nd–Sr isotope space and $^{206}Pb/^{207}Pb$–$^{208}Pb/^{207}Pb$ space that define at least two and probably four end-members. One end-member, with low Sr-high Nd isotope ratios (Fig. 8A) and high $^{206}Pb/^{207}Pb$ and $^{208}Pb/^{207}Pb$ ratios (Fig. 8B) has previously been identified as Antarctic volcanics (Matsumoto and Hinkley, 2001; Vallelonga et al., 2004, 2005, 2010). A second is characterized as a continental non-volcanic dust source with higher Sr-lower Nd-$^{206}Pb/^{207}Pb$–$^{208}Pb/^{207}Pb$ isotope ratios (Fig. 8A and B). Vallelonga et al. (2010) showed that there must also be at least one additional EAIS continental non-volcanic dust source with intermediate $^{206}Pb/^{207}Pb$ and $^{208}Pb/^{207}Pb$ ratios, and consistent with that observation, all of the ice core dust data fall within a mixing envelope bounded by four end-members: West Antarctic Rift System (WARS) volcanics, Patagonia, Tierra del Fuego, and Central Western Argentina in Nd–Sr isotope and $^{206}Pb/^{207}Pb$–$^{208}Pb/^{207}Pb$ space (Fig. 8). Along with the EAIS dust data, representative compositions for the South American PSAs and the WARS volcanic end-member are shown, as are calculated mixing trends. Our estimates of the compositions of potential Antarctic volcanic and South American end-members, based on median values from published data where available, are listed in Table 1.

Next, we apply a combined Sr-Nd-Pb isotope approach to assess NZ as a potential end-member to East Antarctica. In the Nd–Sr and $^{206}Pb/^{207}Pb$–$^{208}Pb/^{207}Pb$ isotope plots (Fig. 8), NZ cannot be precluded as an EAIS dust contributor, because the NZ data lie at the continental dust end of the EAIS Nd–Sr isotope trend and within the $^{206}Pb/^{207}Pb$–$^{208}Pb/^{207}Pb$ data envelope. However, having determined the Nd, Sr, and Pb isotopic compositions of the different PSA end-members (Table 1), we can predict the compositional limits of mixtures in Pb–Nd and Pb–Sr space, something not possible with existing EAIS ice core data because Sr–Nd and Pb isotopes have not been measured on the same samples. In addition, having determined whether the sources are Antarctic volcanics or continent-derived dust, and given some geochemical data on the PSA samples, we are able to estimate the Sr, Nd, and Pb concentrations (Table 1) and to constrain the mixing envelopes (Fig. 9).

This combined Sr-Nd-Pb isotopic approach allows for a robust test of NZ as a potential dust source to the EAIS, even though Pb isotopes were not measured on the same EAIS samples as Sr–Nd isotopes. As the EAIS data fall between the Antarctic volcanics and South American end-members in Nd–Sr and $^{206}Pb/^{207}Pb$–$^{208}Pb/^{207}Pb$ isotope space (Fig. 8), we can expect them to do so in Pb–Nd and Pb–Sr isotope space as well (Fig. 9), as long as the samples measured for Pb isotopes and those measured for Sr–Nd isotopes are both broadly representative of EAIS dust, a reasonable assumption given the large number of data (Figs. 7 and 8). We find that the NZ data fall outside of the inferred South American data envelope (Fig. 9). The data thus indicate that NZ has not been a significant contributor of dust to East Antarctica during glacial climates. Our analysis likewise indicates that the Puna-Altiplano region of South America has played no more than a minor role as a dust source to the EAIS during glacial climates (Fig. 9).

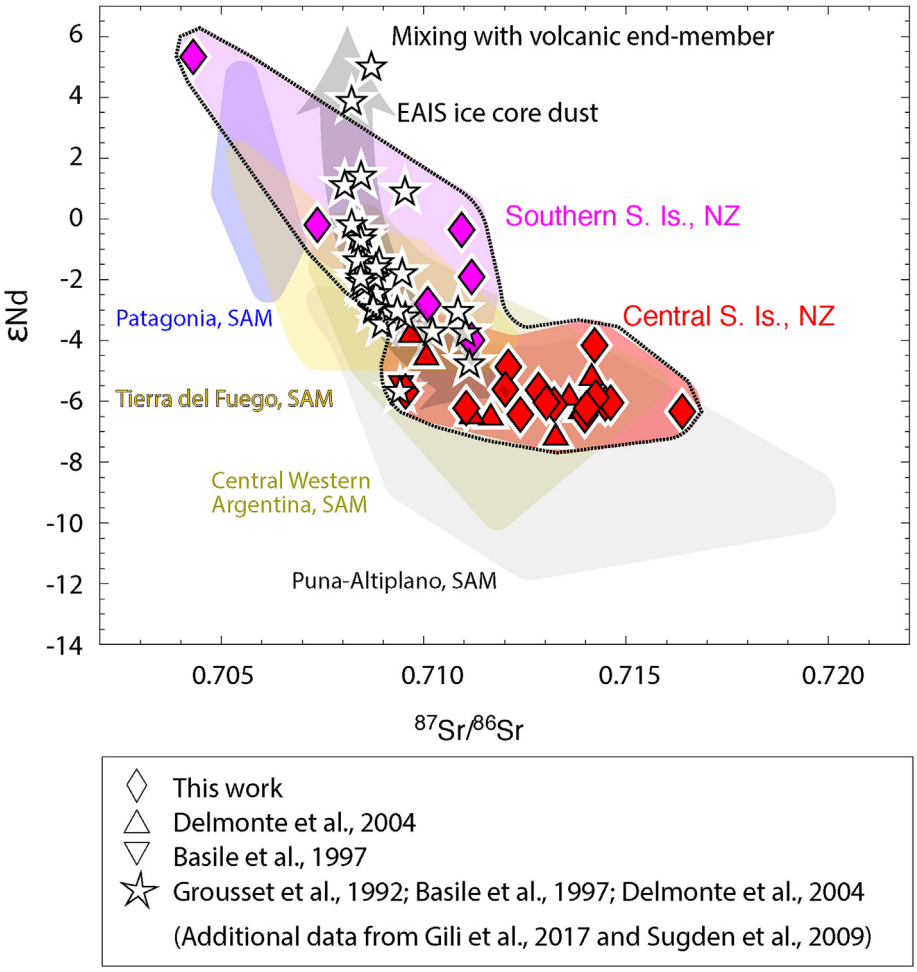

Fig. 7. Comparison of NZ South Island sediments with glacial-age East Antarctic Ice Sheet (EAIS) ice core dust εNd vs. $^{87}Sr/^{86}Sr$. Gray arrow shows potential end-member mixing pathway for ice core dust samples, and colored fields indicate South American PSA regions for reference. Based on these data alone, the NZ South Island cannot be ruled out as an end-member for East Antarctic glacial dust. Error bars are smaller than symbols.

4.4. New Zealand as a source of dust to the South Pacific

The absence of significant NZ dust in East Antarctica might be unsurprising, given the NZ South Island's location at ~170°E longitude and modeled dust transport patterns (described in Section 2.2). Instead, HYSPLIT (Neff and Bertler, 2015) and GCM (Li et al., 2008; Albani et al., 2011) models support the transport of NZ dust to the Pacific sector of the Southern Ocean and to West Antarctica. An assessment of NZ versus Australian sources to this region over the Holocene can be made using the geochemical and isotopic data of core-top samples from 36 cores recovered from 36°S to 70°S between New Zealand and South America (Molina-Kescher et al., 2014; Wengler et al., 2019). We note that these cores span a large geographic range (Fig. 1A, S10) and reflect a wide range of sedimentation rates. The two studies also analyzed different grain size fractions, bulk detritus (Molina-Kescher et al., 2014) and <10 μm diameter (with five samples at <5 μm; Wengler et al., 2019). This size difference may impact the Sr isotopes but is unlikely to affect Nd isotopes (Dasch, 1969; Biscaye and Dasch, 1971; Goldstein et al., 1984; Biscaye et al., 1997; Eisenhauer et al., 1999; Smith et al., 2003; Chen et al., 2007; Gaiero, 2007; Feng et al., 2009; Meyer et al., 2011; Bayon et al., 2015). Molina-Kescher et al. (2014) concluded, based on Sr–Nd isotopes, that the dust is sourced from both NZ and Australia, while Wengler et al. (2019) concluded that NZ is not a significant dust source for that region. Wengler et al. (2019) excluded NZ mainly based on NZ dust samples having high La/Yb compared to the South Pacific core-top samples, using the limited REE data set available at that time and lithogenic flux data from south of New Zealand. We replotted the diagram used to exclude New Zealand, La/Yb vs Eu/Eu*, adding our new data set (Fig. S11). The NZ samples used by Wengler et al. for comparison included dust trap and glacial dust from the west coast of NZ; among these, several samples were previously interpreted as containing 60–90% Australian dust (Marx et al., 2005b), and these have high La/Yb. However, our NZ samples and the NZ loess samples from Marx et al. (2005b) have La/Yb like the South Pacific samples (Fig. S11). Therefore, the La/Yb ratios do not exclude NZ to be a possible dust source. Moreover, several of the Wengler et al. (2019) samples have very low REE concentrations, 1–2 orders of magnitude lower than typical crustal values, resulting in low analytical precision and accuracy. This is evident in the REE plots, which show unrealistic jagged patterns for these samples (Fig S12A). Excluding these data, the REE patterns of the remaining Pacific sector sediments and our NZ sediments are effectively indistinguishable (Fig. 10). In contrast, the Australian-sourced west coast NZ dust samples used by Wengler et al. (2019) to exclude NZ as a dust source do show different REE patterns than our NZ samples and the Pacific core-top sediments (Fig. S12B). Therefore, based on REE patterns and La/Yb ratios, NZ PSAs cannot be ruled out as potential dust sources to the Pacific sector of the Southern Ocean.

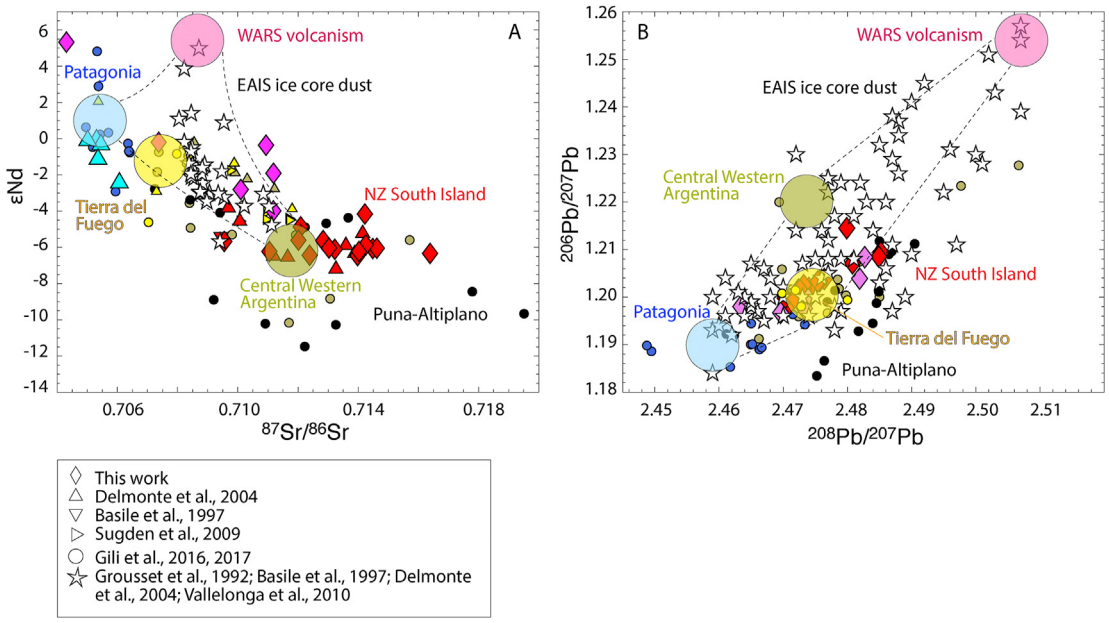

Fig. 8. EAIS glacial-age ice core dust (stars) plotted with NZ and South American sediments (colors as in Figs. 5 and 7), showing inferred end-member compositions required to explain majority of EAIS dust compositions (large colored circles with labels). These compositions (given in Table 1) are used in Fig. 9 to predict mixing in Pb–Nd and Pb–Sr isotope spaces. Dashed lines represent calculated mixing curves between end-member compositions. WARS: West Antarctic Rift System. Error bars are smaller than symbols. (For interpretation of the references to color in this figure legend, the reader is referred to the Web version of this article.)

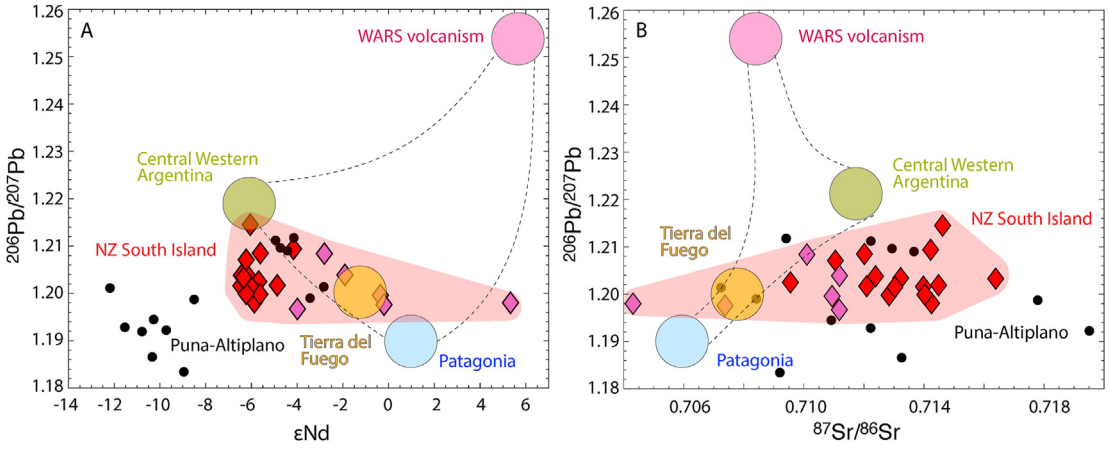

Fig. 9. Predicted mixing patterns (dashed lines) between the four inferred end-members for EAIS glacial-age ice core dust shown in Fig. 11: WARS volcanism, Patagonia, Central Western Argentina, and Tierra del Fuego. NZ South Island and Puna-Altiplano samples plot largely outside the region of inferred mixing, suggesting that neither was a significant dust supplier to the EAIS during glacials. Error bars are smaller than symbols.

Table 1
End-member values used to calculate Sr–Pb and Nd–Pb mixing curves in Fig. 9.

	WARS Volcanism	Central Western Argentina	Tierra del Fuego	Patagonia
$^{206}Pb/^{207}$ Pb	1.26	1.22	1.2	1.19
$^{208}Pb/^{207}$ Pb	2.51	2.475	2.475	2.46
epsNd	6	−6	−1	1
$^{87}Sr/^{86}Sr$	0.709	0.712	0.708	0.706
[Sr]	380	267	260	264
[Nd]	17.2	28	16	20
[Pb]	2.95	26	23	25

(Data from Keller et al., 1992; Luttinen et al., 1998; Gili et al., 2016; 2017; several concentrations estimated where data unavailable).

Sr-Nd-Pb isotope ratios are also compatible with NZ as an important dust source to the Pacific sector. Sr–Nd isotope data show that the NZ South Island was a likely, but not an exclusive, source of dust to these cores. The sediment compositions can be explained by a mixture of South Island and North Island sources (Fig. 11A), with the sediment data enveloped by those of the NZ

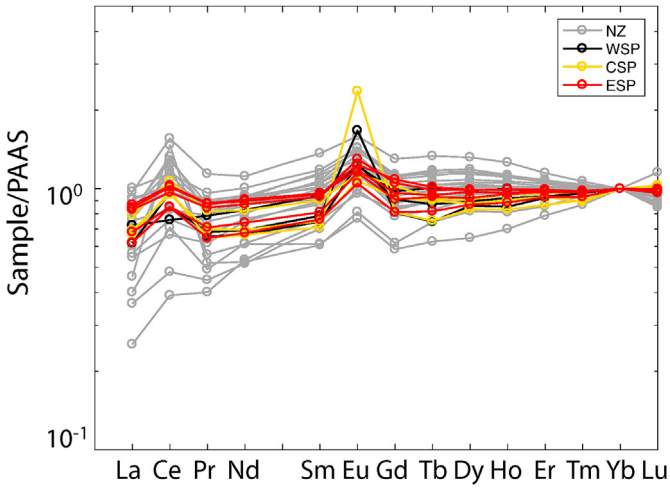

Fig. 10. Rare Earth Element (REE) data from New Zealand (this study) compared to data from the South Pacific, showing similar patterns characterized by relatively flat PAAS-normalized profiles with variable Ce and Eu enrichment. Wengler et al. (2019) samples are colored as in original publication; WSP: western South Pacific; CSP: central South Pacific; ESP: eastern South Pacific. Values are normalized to Post-Archean Australian Shale (PAAS) (Nance and Taylor, 1976; Taylor and McLennan, 1985; Pourmand et al., 2012) and further normalized to Yb.

North and South Island samples. For the NZ North Island, the figure shows published PSA samples (gray triangles, Delmonte et al., 2004) and rock samples, mainly volcanics and some sedimentary rocks, with Sr-Nd-Pb isotope data from the GEOROC database (GEOROC pre-compiled data sets, convergent margins, New_-Zealand.csv), used because there are no published Pb isotope data on the North Island PSA samples. As might be expected, the rock data mostly have even lower $^{87}Sr/^{86}Sr$ and higher εNd than the PSA samples. Given the North Island's abundant volcanic activity over the last ~30 ka (e.g. Lowe et al., 2008), the composition of the Pacific data between the North and South Island fields may indicate contributions from North Island tephra or remobilized ash along with South Island PSAs. It can be seen in Fig. 11A that the Sr–Nd isotopes of South Pacific sediments follow a calculated mixing trend (dashed lines) between the central South Island and the North Island of NZ, consistent with this interpretation (Molina-Kescher et al., 2014; Wengler et al., 2019).

The Pacific sector Sr–Nd isotope data are also consistent with dust contributions from Australia's Darling and Kati Thanda-Lake Eyre Basins (Molina-Kescher et al., 2014; Wengler et al., 2019). While LEB Sr–Nd compositions are similar to the South Pacific core-top data, the LEB sediments tend to have slightly higher εNd and $^{87}Sr/^{86}Sr$ values than the Pacific sediments (inset, Fig. 11A). Although a strong case exists for LEB as a dust source to the Pacific sector based not only on geochemistry but also on modern satellite observations (Wengler et al., 2019), the LEB sediments cannot fully explain the Pacific sediment compositions, as the cluster of core-top data sits largely at lower εNd and $^{87}Sr/^{86}Sr$ values than the LEB sediments, and thus outside the LEB field. Pb isotope data from these source areas can help narrow things down, as Darling Basin sediments have higher $^{208}Pb/^{207}Pb$, higher $^{208}Pb/^{204}Pb$, and lower $^{206}Pb/^{204}Pb$ compared to the South Pacific core-top and NZ sediments (Fig. 11B–D). In contrast, the new LEB Pb data overlap with our NZ data. Therefore, the LEB remains viable as a dust source to the South Pacific based on Sr-Nd-Pb isotopes.

The Pacific sector core sediments plot almost entirely within the NZ-LEB field for all Pb isotope ratios, with the exception of five samples. These exceptions include a core recovered near the NZ continental shelf (Fig. S10; core 105 in Wengler et al., 2019) that is offset geographically from the other samples, with $^{206}Pb/^{207}Pb$ and $^{206}Pb/^{204}Pb$ ratios much higher than the rest of the Pacific samples. Given the proximity to NZ rivers, we suggest these values reflect inclusion of heavy minerals such as zircon, which can cause bulk samples to show high $^{206}Pb/^{204}Pb$ (e.g., Garçon et al., 2014). The other four samples are located between ~58°S-61°S and ~135°W-160°W (shown as white circles in Fig. S10, cores 62, 64, 70, and 84 in Wengler et al., 2019). These also fall outside of the NZ data field (Fig. 11B–D), but to low $^{206}Pb/^{207}Pb$ and $^{206}Pb/^{204}Pb$ ratios (high $^{208}Pb/^{206}Pb$ and $^{207}Pb/^{206}Pb$). Moreover, they follow Pb isotope trends similar to those of Murray-Darling sediments from Australia (De Deckker et al., 2010a). We suggest that these four samples either were influenced by dust from the Murray-Darling region, or that their Pb isotope ratios reflect the presence of Pb from Australia's Broken Hill mine that was extensively used as an additive to gasoline and often taken as an indicator of anthropogenic Pb contamination, which has been discussed for Murray-Darling sediments (Kamber et al., 2010; De Deckker et al., 2010b). Given that the four cores cluster geographically (Fig. S10), their Pb isotope ratios plausibly reflect a mix of sources different from the other cores. Three of these four samples are among those from Wengler et al. (2019) with very low REE abundances (Fig. S12A), and if this is the case with Pb then these samples might be easy to contaminate (Pb concentrations and blank values were not reported). These four samples are located near the main export route of icebergs from the Ross Sea, and may reflect this additional source of lithogenic material (Struve, pers. comm.). However, they form a trend toward the NZ-South Pacific data cluster, consistent with a NZ end-member (Fig. 11B–D). The compositions of these five samples notwithstanding, the rest of the Pacific sector sediment compositions are consistent with a NZ source. Moreover, the new Pb isotope data from LEB also overlap with the field of the South Pacific core-tops, although outside of the field formed by the data of Vallelonga et al. (2010) on the same samples. These differences are presumably related to the different processing of the samples (leached bulk samples vs digested <5 μm fractions as discussed in Section 3.3). Thus Sr-Nd-Pb isotope ratios allow Kati Thanda-Lake Eyre to be a South Pacific source area, provided that atmospheric circulation patterns allow the dust from this region to reach the Pacific sector independent of other Australian sources.

In sum, our new data show that both NZ and LEB are likely dust sources to the Pacific sector of the Southern Ocean during the Holocene. While neither the South Island of NZ nor LEB can serve as an exclusive dust source, given that the South Pacific core-top data form a cluster slightly outside their respective fields, both are viable end-members. Specifically, we argue that Pacific sector core-top sediment compositions can be explained by a mixture of dust and/or ash from the North and South Islands of NZ, along with LEB. The published Pb isotope data from Australian PSAs other than the LEB indicate that they are not major contributors to most Pacific sector sediment samples. Marine sediment cores from the Pacific sector show a three-fold increase in dust deposition during glacial climates, potentially reflecting enhanced glaciogenic dust production from NZ (Lamy et al., 2014), or dust input from other regions. We expect that NZ's role as a dust source to the Pacific sector was enhanced during glacial climates.

5. Conclusions

Abundant evidence exists of NZ's dustiness and prolific sediment production during the LGM and past glacials, both in widespread terrestrial loess deposits and in offshore cores (Bal, 1996; Eden and Hammond, 2003). Outwash plains, such as those that were exposed on the eastern side of the South Island downstream from actively eroding glaciers, serve as important dust emissions

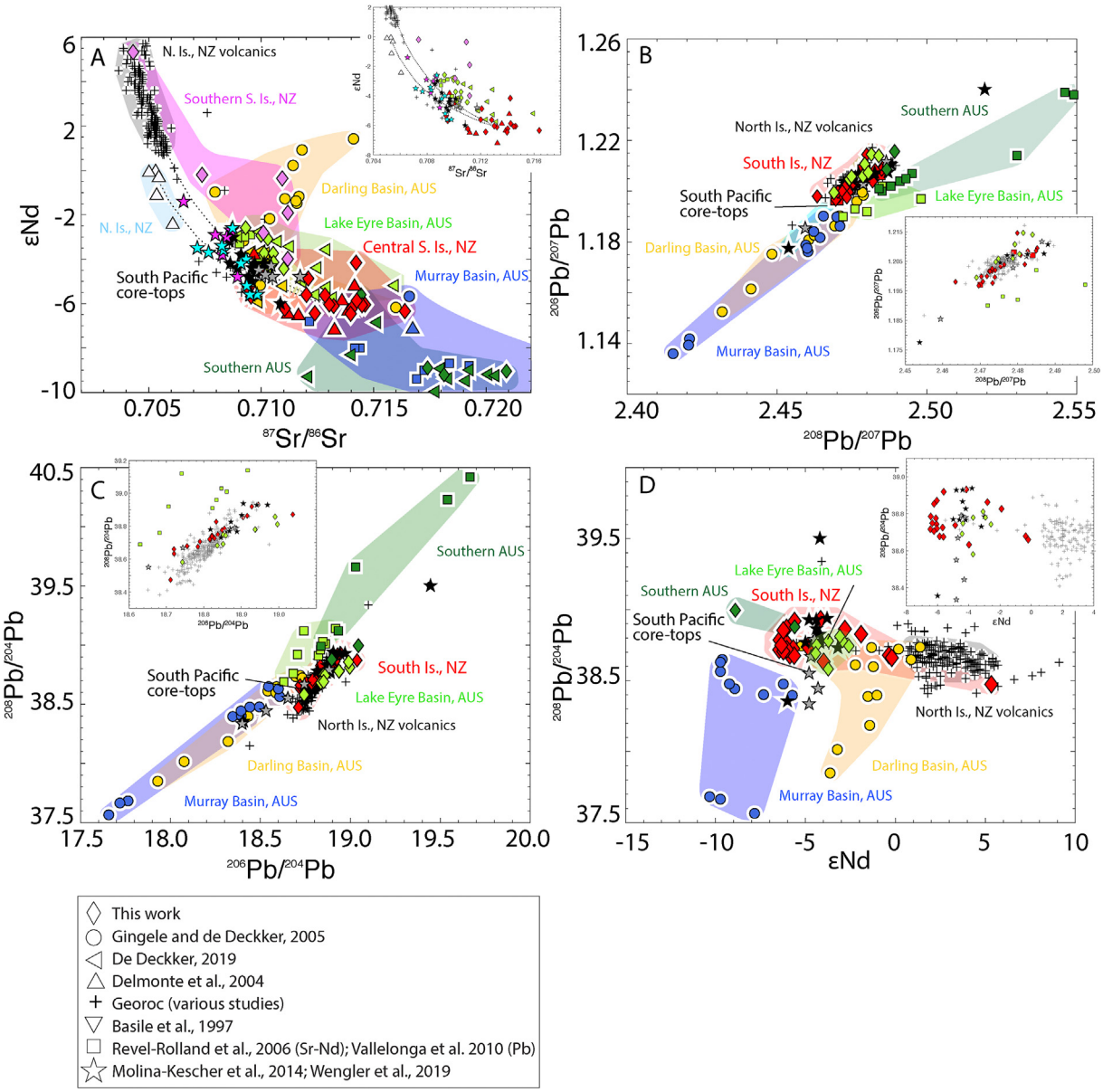

Fig. 11. Comparison of South Pacific sediment isotope compositions with NZ and Australian (AUS) fine-grained (<5 μm) sediments. A) εNd vs. $^{87}Sr/^{86}Sr$. Black and gray stars represent core-top data from Wengler et al. (2019; gray points indicate low REE concentrations), while magenta and cyan stars show points from Molina-Kescher et al. (2014) (magenta points are <40° S; cyan are >40° S; see Fig. S10 for map of core locations). Given the limited data on sediments available from the North Island of NZ, we include bedrock data available through the GeoRoc database to characterize the volcanic end-member. South Pacific sediments can be explained by a mixture of South and North Island, NZ dust and/or ash (dotted lines represent mix of central South Island and North Island sediments and volcanic materials, respectively), along with LEB sediments. B) $^{206}Pb/^{207}Pb$ vs. $^{208}Pb/^{207}Pb$. C) $^{206}Pb/^{204}Pb$ vs. $^{208}Pb/^{204}Pb$. D) $^{208}Pb/^{204}Pb$ vs. εNd. South Pacific sediments lie within the Pb–Pb field defined by the South and North Islands of NZ, except for four samples, which overlap sediments from the Murray-Darling Basin of Australia (see text). Insets in each panel show data points for regions considered most relevant to interpreting the Pacific core-top data. (For interpretation of the references to color in this figure legend, the reader is referred to the Web version of this article.)

regions (Prospero et al., 2012). We estimate the expansion of glacial outwash plains based on a sea level lowering of 130 m at the LGM (Osterberg, 2006), and find that the Canterbury Plains likely covered ~38,500 km^2 (an increase of ~30,000 km^2 relative to today; Leckie, 2003). Moreover, due to a lower sea level, the Southland/southern Otago region may also have expanded to 50,500 km^2 (an increase of ~45,000 km^2 relative to today; see section 4.2), extending NZ's land mass southward into the path of the westerlies. Considering NZ's extreme uplift and erosion rates (~10 m kyr^{-1}), we suggest that the South Island, though limited in extent compared to larger southern landmasses, likely served as an important dust source to the high latitudes of the Southern Hemisphere.

We present Sr-Nd-Pb isotope and major/trace element data of fine-grained sediments (including loess, glaciogenic materials, and modern river silts) for the purpose of characterizing NZ's South Island as a source of dust and fine-grained sediment to the high-latitude atmosphere and ocean. We find significant isotopic variations corresponding to differences in crust formation ages between the central and southern regions of the South Island. The central region (Canterbury Plains) is easily distinguished from the southern region by having more negative εNd and lower $^{207}Pb/^{204}Pb$, and generally higher $^{87}Sr/^{86}Sr$. There is no relationship between Sr, Nd, or Pb isotopic ratios and the CIA weathering index in samples or the age of samples deposited over the past ~80 ka.

Using a combination of Sr-Nd-Pb isotope ratios, we show that the NZ South Island can be distinguished geochemically from many Southern Hemisphere dust sources. A key finding is that Sr-Nd-Pb isotopes can help to discriminate NZ from southern Africa, regions of South America south of ~37°S (i.e., Patagonia and Tierra del Fuego), and many sources in Australia. However, geochemical similarities between the NZ South Island and more northerly regions of South America, including Central Western Argentina (including the Pampas) and the Puna-Altiplano Plateau, somewhat hinder downstream source attribution. Nevertheless, our evaluation indicates that Pb–Nd and Pb–Sr isotopes are the most effective discriminants for NZ versus South American sources. Moreover, we present new Sr-Nd-Pb isotope data on PSA samples from the Kati Thanda-Lake Eyre Basin that show major overlap with the NZ South Island.

By determining the compositional range of possible mixtures of NZ, South American and Antarctic sources, we find that East Antarctic ice core dust samples fall within a mixing envelope defined by WARS volcanism and key South American dust sources. The NZ samples fall outside this envelope, and we conclude that NZ is not a major dust source for East Antarctica. In contrast, using REEs and Sr-Nd-Pb isotopes, we demonstrate that the NZ South and North Islands together can explain the dust delivered to the Pacific sector of the Southern Ocean during the Holocene, with potential contributions from LEB as well. With the exception of four geographically related samples, Holocene South Pacific sediments are consistent with these sources, and do not require the contribution of any other source material. Therefore, we conclude that NZ should be considered as a source of glaciogenic dust to the Pacific sector of the Southern Ocean, and by extension West Antarctica, during glacial climates and through the Holocene.

Author statement

Bess G. Koffman: Conceptualization, Investigation, Methodology, Data curation, Writing - original draft, Writing - review & editing, Visualization, Funding acquisition; Steven L. Goldstein: Conceptualization, Methodology, Writing - review & editing, Funding acquisition; Gisela Winckler: Conceptualization, Methodology, Writing - review & editing; Alejandra Borunda: Investigation; Michael R. Kaplan: Conceptualization, Methodology, Writing - review & editing; Louise Bolge: Investigation, Methodology; Yue Cai: Investigation, Methodology; Cristina Recasens: Investigation, Methodology; Tobias N. B. Koffman: Resources; Paul Vallelonga: Resources, Methodology

Declaration of competing interest

The authors declare that they have no known competing financial interests or personal relationships that could have appeared to influence the work reported in this paper.

Acknowledgements

We thank Christopher Moy for generously providing a loess sample from Oamaru. We appreciate help in the field and with GIS from Noah Pollock. Thanks also go to Jonathan Chipman and Steve Gaughan, who provided help with GIS analysis. Our field sampling approach benefited from conversations with David Barrell and Aaron Putnam. Trevor Williams and Bob Hawley helped with GMT. We thank Torben Struve for discussions about the South Pacific core data. Thanks also go to Peter Koons, who helped inspire this work by asking "what about New Zealand?" This project was largely supported by an NSF Postdoctoral Fellowship (NSF ANT–1204050) as well as by a Dartmouth Society of Fellows Postdoctoral Fellowship to B.G.K, and by the Storke Endowment of the Department of Earth and Environmental Sciences of Columbia University. This is LDEO publication #8457. Data from this paper are available through the EarthChem data repository at the following link: https://doi.org/10.26022/IEDA/111726.

Appendix A. Supplementary data

Supplementary data to this article can be found online at https://doi.org/10.1016/j.quascirev.2020.106659.

References

Aarons, S., Aciego, S., Gabrielli, P., Delmonte, B., Koornneef, J., Wegner, A., Blakowski, M., 2016. The impact of glacier retreat from the Ross Sea on local climate: characterization of mineral dust in the Taylor Dome ice core, East Antarctica. Earth Planet Sci. Lett. 444, 34–44.

Aarons, S.M., Aciego, S.M., Arendt, C.A., Blakowski, M.A., Steigmeyer, A., Gabrielli, P., Sierra-Hernández, M.R., Beaudon, E., Delmonte, B., Baccolo, G., May, N.W., Pratt, K.A., 2017. Dust composition changes from Taylor Glacier (East Antarctica) during the last glacial-interglacial transition: a multi-proxy approach. Quat. Sci. Rev. 162, 60–71.

Albani, S., Mahowald, N.M., Delmonte, B., Maggi, V., Winckler, G., 2011. Comparing modeled and observed changes in mineral dust transport and deposition to Antarctica between the Last Glacial Maximum and current climates. Clim. Dynam. 38, 1731–1755.

Alloway, B.V., Lowe, D.J., Barrell, D.J.A., Newnham, R.M., Almond, P.C., Augustinus, P.C., Bertler, N.A.N., Carter, L., Litchfield, N.J., McGlone, M.S., Shulmeister, J., Vandergoes, M.J., Williams, P.W., 2007. Towards a climate event stratigraphy for New Zealand over the past 30 000 years (NZ-INTIMATE project). J. Quat. Sci. 22, 9–35.

Andrews, J.T., Tedesco, K., 1992. Detrital carbonate-rich sediments, northwestern Labrador Sea: implications for ice-sheet dynamics and iceberg rafting (Heinrich) events in the North Atlantic. Geology 20, 1087–1090.

Bal, A.A., 1996. Valley fills and coastal cliffs buried beneath an alluvial plain: evidence from variation of permeabilities in gravel aquifers, Canterbury Plains, New Zealand. Journal of Hydrology. New Zealand 35, 1–27.

Barrell, D.J.A., 2011. Quaternary glaciers of New Zealand. In: Ehlers, J., Gibbard, P., Hughes, P. (Eds.), Developments in Quaternary Science. Elsevier, pp. 1047–1064.

Barrell, D.J.A., Andersen, B.G., Denton, G.H., 2011. Glacial Geomorphology of the Central South Island, New Zealand, vol. 27. GNS Science monograph, p. 81 p + map (85 sheets) + legend (81 sheet). Lower Hutt, New Zealand. GNS Science. 81:100,000-scale geomorphology map; provisional digital data, as at [101 September 2011].

Basile, I., Grousset, F.E., Revel, M., Petit, J.R., Biscaye, P.E., Barkov, N.I., 1997. Patagonian origin of glacial dust deposited in East Antarctica (Vostok and Dome C) during glacial stages 2, 4 and 6. Earth Planet Sci. Lett. 146, 573–589.

Bayon, G., Toucanne, S., Skonieczny, C., Andre, L., Bermell, S., Cheron, S., Dennielou, B., Etoubleau, J., Freslon, N., Gauchery, T., Germain, Y., Jorry, S.J., Menot, G., Monin, L., Ponzevera, E., Rouget, M.-L., Tachikawa, K., Barrat, J.A., 2015. Rare earth elements and neodymium isotopes in world river sediments revisited. Geochem. Cosmochim. Acta 170, 17–38.

Berger, G.W., Pillans, B.J., Bruce, J.G., McIntosh, P.D., 2002. Luminescence chronology of loess-paleosol sequences from southern South Island, New Zealand. Quat. Sci. Rev. 21, 1899–1913.

Biscaye, P.E., 1965. Mineralogy and sedimentation of recent deep-sea clay in the Atlantic Ocean and adjacent seas and oceans. GSA Bulletin 76, 803–832.

Biscaye, P.E., Dasch, E.J., 1971. The rubidium, strontium, strontium-isotope system in deep-sea sediments: Argentine Basin. J. Geophys. Res. 76, 5087–5096.

Biscaye, P.E., Grousset, F.E., Revel, M., Van der Gaast, S., Zielinski, G.A., Vaars, A., Kukla, G., 1997. Asian provenance of glacial dust (stage 2) in the Greenland Ice Sheet Project 2 ice core, Summit, Greenland. J. Geophys. Res. 102 (26).

Blum, A.E., 1994. Feldspars in Weathering, Feldspars and Their Reactions. Springer, pp. 595–630.

Blum, J.D., Erel, Y., 1997. Rb Sr isotope systematics of a granitic soil chronosequence: the importance of biotite weathering. Geochem. Cosmochim. Acta 61, 3193–3204.

Bokhari, S.N.H., Meisel, T.C., 2017. Method development and optimisation of sodium peroxide sintering for geological samples. Geostand. Geoanal. Res. 41, 181–195.

Bullard, J.E., Austin, M.J., 2011. Dust generation on a proglacial floodplain, West Greenland. Aeolian Research 3, 43–54.

Chen, J., Li, G., Yang, J., Rao, W., Lu, H., Balsam, W., Sun, Y., Ji, J., 2007. Nd and Sr isotopic characteristics of Chinese deserts: implications for the provenances of Asian dust. Geochem. Cosmochim. Acta 71, 3904–3914.

Cogez, A., Meynadier, L., Allegre, C., Limmois, D., Herman, F., Gaillardet, J., 2015. Constraints on the role of tectonic and climate on erosion revealed by two time series analysis of marine cores around New Zealand. Earth Planet Sci. Lett. 410, 174–185.

Cox, S.C., Barrell, D.J.A., 2007. Geology of the Aoraki Area. Institute of Geological and Nuclear Sciences, Lower Hutt, New Zealand, 1:250000 geological map.

Craw, D., Kerr, G., Reith, F., Falconer, D., 2015. Pleistocene paleodrainage and placer

gold redistribution, western Southland, New Zealand. N. Z. J. Geol. Geophys. 58, 137–153.
Dasch, E.J., 1969. Strontium isotopes in weathering profiles, deep-sea sediments, and sedimentary rocks. Geochem. Cosmochim. Acta 33, 1521–1552.
De Deckker, P., 2019. An evaluation of Australia as a major source of dust. Earth Sci. Rev. 194, 536–567.
De Deckker, P., 2020. Airborne dust traffic from Australia in modern and Late Quaternary times. Global Planet. Change 184, 103056.
Delmonte, B., Andersson, P.S., Schoberg, H., Hansson, M., Petit, J.R., Delmas, R., Gaiero, D.M., Maggi, V., Frezzotti, M., 2010. Geographic provenance of aeolian dust in East Antarctica during Pleistocene glaciations: preliminary results from Talos Dome and comparison with East Antarctic and new Andean ice core data. Quat. Sci. Rev. 29, 256–264.
Delmonte, B., Basile-Doelsch, I., Petit, J.R., Maggi, V., Revel-Rolland, M., Michard, A., Jagoutz, E., Grousset, F., 2004. Comparing the Epica and Vostok dust records during the last 220,000 years: stratigraphical correlation and provenance in glacial periods. Earth Sci. Rev. 66, 63–87.
Delmonte, B., Petit, J.R., Basile-Doelsch, I., Jagoutz, E., Maggi, V., 2007. Late quaternary interglacials in East Antarctica from ice-core dust records. In: Sirocko, F., Claussen, M., Sanchez-Goni, M.F., Litt, T. (Eds.), The Climate of Past Interglacials. Elsevier, Amsterdam, pp. 53–73.
Denton, G.H., Anderson, R.F., Toggweiler, J.R., Edwards, R.L., Schaefer, J.M., Putnam, A.E., 2010. The last glacial termination. Science 328, 1652–1656.
Eden, D.N., Hammond, A.P., 2003. Dust accumulation in the New Zealand region since the last glacial maximum. Quat. Sci. Rev. 22, 2037–2052.
Eisenhauer, A., Meyer, H., Rachold, V., Tutken, T., Wiegand, B., Hansen, B.T., Spielhagen, R.F., Lindemann, F., Kassens, H., 1999. Grain size separation and sediment mixing in Arctic Ocean sediments: evidence from the strontium isotope systematic. Chem. Geol. 158, 173–188.
Farmer, G.L., Barber, D.C., Andrews, J.T., 2003. Provenance of late quaternary ice-proximal sediments in the north atlantic: Nd, Sr, and Pb isotopic evidence. Earth Planet Sci. Lett. 209, 227–243.
Feng, J.-L., Zhu, L.-P., Zhen, X.-L., Hu, Z.-G., 2009. Grain size effect on Sr and Nd isotopic compositions in eolian dust: implications for tracing dust provenance and Nd model age. Geochem. J. 43, 123–1313.
Fischer, H., Siggaard-Andersen, M.-L., Ruth, U., Rothlisberger, R., Wolff, E., 2007. Glacial/interglacial changes in mineral dust and sea-salt records in polar ice cores: sources, transport, and deposition. Rev. Geophys. 45.
Frost, C.D., Coombs, D.S., 1989. Nd isotope character of New Zealand sediments: implications for terrane concepts and crustal evolution. Am. J. Sci. 289, 744–770.
Gaiero, D.M., 2007. Dust provenance in Antarctic ice during glacial periods: from where in southern South America? Geophys. Res. Lett. 34.
Gaiero, D.M., Brunet, F., Probst, J.-L., Depetris, P.J., 2007. A uniform isotopic and chemical signature of dust exported from Patagonia: rock sources and occurrence in southern environments. Chem. Geol. 238, 107–120.
Gaiero, D.M., Depetris, P.J., Probst, J.-L., Bidart, S.M., Leleyter, L., 2004. The signature of river- and wind-borne materials exported from Patagonia to the southern latitudes: a view from REEs and implications for paleoclimatic interpretations. Earth Planet Sci. Lett. 219, 357–376.
Gallet, S., Jahn, B., Torii, M., 1996. Geochemical characterization of the Luochuan loess-paleosol sequence, China, and paleoclimatic implications. Chem. Geol. 133, 67–88.
Garçon, M., Chauvel, C., France-Lanord, C., Limonta, M., Garzanti, E., 2014. Which minerals control the Nd-Hf-Sr-Pb isotopic compositions of river sediments? Chem. Geol. 364, 42–55.
Gili, S., Gaiero, D.M., Goldstein, S.L., Chemale Jr., F., Jweda, J., Kaplan, M.R., Becchio, R.A., Koester, E., 2017. Glacial/interglacial changes of Southern Hemisphere wind circulation from the geochemistry of South American dust. Earth Planet Sci. Lett. 469, 98–109.
Gili, S., Gaiero, D.M., Goldstein, S.L., Chemale Jr., F., Koester, E., Jweda, J., Vallelonga, P., Kaplan, M.R., 2016. Provenance of dust to Antarctica: a lead isotopic perspective. Geophys. Res. Lett. 43, 2291–2298.
Gingele, F.X., De Deckker, P., 2005. Clay mineral, geochemical and Sr-Nd isotopic fingerprinting of sediments in the Murray-Darling fluvial sytem, southeast Australia. Aust. J. Earth Sci. 52, 965–974.
GNS, 2004. Geological Map of New Zealand. Institute of Geological and Nuclear Sciences, Lower Hutt, New Zealand.
Goldstein, S.L., O'Nions, R.K., Hamilton, P.J., 1984. A Sm-Nd isotopic study of atmospheric dusts and particulates from major river systems. Earth Planet Sci. Lett. 70, 221–236.
Golledge, N.R., Mackintosh, A.N., Anderson, B.M., Buckley, K.M., Doughty, A.M., Barrell, D.J., Denton, G.H., Vandergoes, M.J., Andersen, B.G., Schaefer, J.M., 2012. Last glacial maximum climate in New Zealand inferred from a modelled southern Alps icefield. Quat. Sci. Rev. 46, 30–45.
Grousset, F., Parra, M., Bory, A., Martinez, P., Bertrand, P., Shimmield, G., Ellam, R.M., 1998. Saharan wind regimes traced by the Sr-Nd isotopic composition of subtropical Atlantic sediments: last Glacial Maximum vs today. Quat. Sci. Rev. 17, 395–409.
Grousset, F.E., Biscaye, P.E., 2005. Tracing dust sources and transport patterns using Sr, Nd and Pb isotopes. Chem. Geol. 222, 149–167.
Grousset, F.E., Biscaye, P.E., Revel, M., Petit, J.-R., Pye, K., Joussaume, S., Jouzel, J., 1992. Antarctic (Dome C) ice-core dust at 18 k.y. B. P.: isotopic constraints on origins. Earth Planet Sci. Lett. 111, 175–182.
Gulick, S.P.S., Jaeger, J.M., Mix, A.C., Asahi, H., Bahlburg, H., Belanger, C.L., Berbel, G.B.B., Childress, L., Cowan, E., Drab, L., Forwick, M., Fukumura, A., Ge, S., Gupta, S., Kioka, A., Konno, S., LeVay, L.J., Marz, C., Matsuzaki, K.M., McClymont, E.L., Moy, C.M., Mueller, J., Nakamura, A., Ojima, T., Ribeiro, F.R., Ridgway, K.D., Romero, O.E., Slagle, A.L., Stoner, J.S., St-Onge, G., Suto, I., Walczak, M.D., Worthington, L.L., Bailey, I., Enkelmann, E., Reece, R., Swartz, J.M., 2015. Mid-Pleistocene Climate Transition Drives Net Mass Loss from Rapidly Uplifting St. Elias Mountains, Alaska. Proceedings of the National Academy of Sciences of the United States of America.
Hemming, S.R., 2004. Heinrich events: massive late Pleistocene detritus layers of the North Atlantic and their global climate imprint. Rev. Geophys. 42.
Hemming, S.R., Bond, G.C., Broecker, W.S., Sharp, W.D., Klas-Mendelson, M., 2000. Evidence from 40Ar/39Ar ages of individual hornblende grains for varying Laurentide sources of iceberg discharges 22,000 to 10,500 yr B.P. Quat. Res. 54, 372–383.
Hemming, S.R., Broecker, W.S., Sharp, W.D., Bond, G.C., Gwiazda, R.H., McManus, J.F., Klas, M., Hajdas, I., 1998. Provenance of Heinrich layers in core V28-82, northeastern Atlantic: 40Ar/39Ar ages of ice-rafted hornblende, Pb isotopes in feldspar grains, and Nd-Sr-Pb isotopes in the fine sediment fraction. Earth Planet Sci. Lett. 164, 317–333.
Hemming, S.R., Hall, C.M., Biscaye, P.E., Higgins, S.M., Bond, G.C., McManus, J.F., Barber, D.C., Andrews, J.T., Broecker, W.S., 2002. 40Ar/39Ar ages and 40Ar* concentrations of fine-grained sediment fractions from North Atlantic Heinrich layers. Chem. Geol. 182, 583–603.
Herman, F., Rhodes, E.J., Braun, J., Heiniger, L., 2010. Uniform erosion rates and relief amplitude during glacial cycles in the Southern Alps of New Zealand, as revealed from OSL-thermochronology. Earth Planet Sci. Lett. 297, 183–189.
Hesse, P.P., 1994. The record of continental dust from Australia in Tasman Sea sediments. Quat. Sci. Rev. 13, 257–272.
Hovius, N., Stark, C.P., Allen, P.A., 1997. Sediment flux from a mountain belt derived by landslide mapping. Geology 25, 231–234.
Jacobsen, S.B., Wasserburg, G.J., 1980. Sm-Nd isotopic evolution of chondrites. Earth Planet Sci. Lett. 50, 139–155.
Jarvis, A., Reuter, H., Nelson, A. and Guevara, E. (2008) Hole-filled Shuttle Radar Topography Mission (SRTM) for the Globe Version 4. Consultative Group on International Agricultural Research-Consortium for Spatial Information (CGIAR-CSI), Washington, DC Available from: http://srtm. csi. cgiar. org (accessed May 2013).
Jickells, T.D., An, Z.S., Andersen, K.K., Baker, A.R., Bergametti, G., Brooks, N., Cao, J.J., Boyd, P.W., Duce, R.A., Hunter, K.A., Kawahata, H., Kubilay, N., laRoche, J., Liss, P.S., Mahowald, N., Prospero, J.M., Ridgwell, A.J., Tegen, I., Torres, R., 2005. Global iron connections between desert dust, ocean biogeochemistry, and climate. Science 308, 67–71.
Kalnay, E., Kanamitsu, M., Kistler, R., Collins, W., Deaven, D., Gandin, L., Iredell, M., Saha, S., White, G., Woolen, J., Zhu, Y., Leetmaa, A., Reynolds, R.L., Chelliah, M., Ebisuzaki, W., Higgins, W., Janowiak, J., Mo, K.C., Ropelewski, C., Wang, J., Jenne, R., Joseph, D., 1996. The NCEP/NCAR 40-year reanalysis product. Bull. Am. Meteorol. Soc. 77, 437–471.
Keller, R.A., Fisk, M.R., White, W.M., Birkenmajer, K., 1992. Isotopic and trace element constraints on mixing and melting models of marginal basin volcanism, Bransfield Strait, Antarctica. Earth Planet Sci. Lett. 111, 287–303.
Kennedy, D.M., Tannock, K.L., Crozier, M.J., Rieser, U., 2007. Boulders of MIS 5 age deposited by a tsunami on the coast of Otago, New Zealand. Sediment. Geol. 200, 222–231.
Kohfeld, K.E., Graham, R.M., de Boer, A.M., Sime, L.C., Wolff, E.W., Le Quéré, C., Bopp, L., 2013. Southern Hemisphere westerly wind changes during the Last Glacial Maximum: paleo-data synthesis. Quat. Sci. Rev. 68, 76–95.
Lamy, F., Gersonde, R., Winckler, G., Esper, O., Jaeschke, A., Kuhn, G., Ullermann, J., Martínez-Garcia, A., Lambert, F., Kilian, R., 2014. Increased dust deposition in the Pacific Southern Ocean during glacial periods. Science 343, 403–407.
Leckie, D.A., 2003. Modern environments of the Canterbury Plains and adjacent offshore areas, New Zealand — an analog for ancient conglomeratic depositional systems in nonmarine and coastal zone settings. Bull. Can. Petrol. Geol. 51, 389–425.
Li, F., Ginoux, P., Ramaswamy, V., 2008. Distribution, transport, and depositon of mineral dust in the Southern Ocean and Antarctica: contribution of major sources. J. Geophys. Res. 113.
Lowe, D.J., Shane, P.A.R., Alloway, B.V., Newnham, R.M., 2008. Fingerprints and age models for widespread New Zealand tephra marker beds erupted since 30,000 years ago: a framework for NZ-INTIMATE. Quat. Sci. Rev. 27, 95–126.
Luttinen, A., Rämö, O., Huhma, H., 1998. Neodymium and strontium isotopic and trace element composition of a Mesozoic CFB suite from Dronning Maud Land, Antarctica: implications for lithosphere and asthenosphere contributions to Karoo magmatism. Geochem. Cosmochim. Acta 62, 2701–2714.
Marx, S.K., Kamber, B.S., McGowan, H.A., 2005a. Estimates of Australian dust flux into New Zealand: quantifying the eastern Australian dust plume pathway using trace element calibrated 210Pb as a monitor. Earth Planet Sci. Lett. 239, 336–351.
Marx, S.K., Kamber, B.S., McGowan, H.A., 2005b. Provenance of long-travelled dust determined with ultra-trace-element composition: a pilot study with samples from New Zealand glaciers. Earth Surf. Process. Landforms 30, 699–716.
Matsumoto, A., Hinkley, T.K., 2001. Trace metal suites in Antarctic pre-industrial ice are consistent with emissions from quiescent degassing of volcanoes worldwide. Earth Planet Sci. Lett. 186, 33–43.
McCraw, J.D., 1975. Quaternary Airfall Deposits of New Zealand, vol. 13. Royal Society of New Zealand Bulletin, pp. 35–44.

McGowan, H.A., Kamber, B., McTainsh, G.H., Marx, S.K., 2005. High resolution provenancing of long travelled dust deposited on the Southern Alps, New Zealand. Geomorphology 69, 208–221.
McGowan, H.A., McTainsh, G.H., Zawar-Reza, P., Sturman, A.P., 2000. Identifying regional dust transport pathways: application of kinematic trajectory modelling to a trans-Tasman case. Earth Surf. Process. Landforms 25, 633–647.
McLennan, S.M., Hemming, S.R., McDaniel, D.K., Hanson, G.N., 1993. Geochemical approaches to sedimentation, provenance, and tectonics. GSA Special Papers 284, 21–40.
Meyer, I., Davies, G.R., Stuut, J.-B.W., 2011. Grain size control on Sr-Nd isotope provenance studies and impact on paleoclimate reconstructions: an example from deep-sea sediments offshore NW Africa. G-cubed 12.
Moore, C.M., Mills, M.M., Achterberg, E.P., Geider, R.J., LaRoche, J., Suggett, D.J., Ussher, S.J., Woodward, E.M.S., 2009. Large-scale distribution of Atlantic nitrogen fixation controlled by iron availability. Nat. Geosci. 2, 867–871.
Mortimer, N., Roser, B.P., 1992. Geochemical evidence for the position of the caples-torlese boundary in the Otago schist, New Zealand. Journal of the Geological Society of London 149, 967–977.
Muhs, D.R., Bush, C.A., Stewart, K.C., Rowland, T.R., Crittenden, R.C., 1990. Geochemical evidence of Saharan dust parent material for soils developed on Quaternary limestones of Caribbean and western Atlantic islands. Quat. Res. 33, 157–177.
Nakai, S., Halliday, A.N., Rea, D.K., 1993. Provenance of dust in the Pacific Ocean. Earth Planet Sci. Lett. 119, 143–157.
Nance, W.B., Taylor, S., 1976. Rare earth element patterns and crustal evolution—I. Australian post-Archean sedimentary rocks. Geochem. Cosmochim. Acta 40, 1539–1551.
Neff, P.D., Bertler, N.A.N., 2015. Trajectory modeling of modern dust transport to the Southern Ocean and Antarctica. J. Geophys. Res.: Atmosphere 120, 9303–9322.
Nesbitt, H., Young, G., 1982. Early Proterozoic climates and plate motions inferred from major element chemistry of lutites. Nature 299, 715–717.
Norris, R.J., Cooper, A.F., 2000. Late Quaternary slip rates and slip partitioning on the Alpine Fault, New Zealand. J. Struct. Geol. 23, 507–520.
Osterberg, E.C., 2006. Late Quaternary (marine isotope stages 6-1) seismic sequence stratigraphic evolution of the Otago continental shelf, New Zealand. Mar. Geol. 229, 159–178.
Paytan, A., Mackey, K.R.M., Chen, Y., Lima, I.D., Doney, S.C., Mahowald, N., Labiosa, R., Post, A.F., 2009. Toxicity of atmospheric aerosols on marine phytoplankton. Proc. Natl. Acad. Sci. U.S.A. 106, 4601–4605.
Porter, S.C., 1975. Equilibrium-line altitudes of late quaternary glaciers in the southern Alps, New Zealand. Quat. Res. 5, 27–47.
Pourmand, A., Dauphas, N., Ireland, T.J., 2012. A novel extraction chromatography and MC-ICP-MS technique for rapid analysis of REE, Sc and Y: revising CI-chondrite and Post-Archean Australian Shale (PAAS) abundances. Chem. Geol. 291, 38–54.
Prospero, J.M., Bullard, J.E., Hodgkins, R., 2012. High-latitude dust over the North Atlantic: inputs from Icelandic proglacial dust storms. Science 335.
Putnam, A.E., Schaefer, J.M., Denton, G.H., Barrell, D.J.A., Andersen, B.G., Koffman, T.N.B., Rowan, A.V., Finkel, R., Rood, D.H., Schwartz, R., Vandergoes, M.J., Plummer, M.A., Brocklehurst, S.H., Kelley, S.E., Ladig, K.L., 2013. Warming and glacier recession in the Rakaia valley, southern Alps of New Zealand, during Heinrich stadial 1. Earth Planet Sci. Lett. 382, 98–110.
Raeside, J.D., 1964. Loess deposits of the South Island, New Zealand, and soils formed on them. N. Z. J. Geol. Geophys. 7, 811–838.
Revel-Rolland, M., De Deckker, P., Delmonte, B., Hesse, P.P., Magee, J.W., Basile-Doelsch, I., Grousset, F., Bosch, D., 2006. Eastern Australia: a possible source of dust in East Antarctica interglacial ice. Earth Planet Sci. Lett. 249, 1–13.
Roser, B.P., Korsch, R.J., 1999. Geochemical characterization, evolution and source of a Mesozoic accretionary wedge: the Torlesse terrane, New Zealand. Geol. Mag. 136, 493–512.
Rowan, A.V., Roberts, H.M., Jones, M.A., Duller, G.A.T., Covey-Crump, S.J., Brocklehurst, S.H., 2012. Optically stimulatd luminescence dating of glacio-fluvial sediments on the Canterbury Plains, South Island, New Zealand. Quat. Geochronol. 8, 10–22.
Rudnick, R., Gao, S., 2003. Composition of the continental crust. The crust 3, 1–64.
Schroth, A.W., Crusius, J., Sholkovitz, E.R., Bostick, B.C., 2009. Iron solubility driven by speciation in dust sources to the ocean. Nat. Geosci. 2.
Shoenfelt, E.M., Sun, J., Winckler, G., Kaplan, M.R., Borunda, A.L., Farrell, K.R., Moreno, P.I., Gaiero, D.M., Recasens, C., Sambrotto, R.N., Bostick, B.C., 2017. High particulate iron(II) content in glacially sourced dusts enhances productivity of a model diatom. Science Advances 3.
Shoenfelt, E.M., Winckler, G., Lamy, F., Anderson, R.F., Bostick, B.C., 2018. Highly bioavailable dust-borne iron delivered to the Southern Ocean during glacial periods. Proc. Natl. Acad. Sci. Unit. States Am. 115, 11180.
Smith, J., Vance, D., R A, K., Archer, C., Toms, P., King, M., Zarate, M., 2003. Isotopic constraints on the source of Argentinian loess - with implications for atmospheric circulation and the provenance of Antarctic dust during recent glacial maxima. Earth Planet Sci. Lett. 212, 181–196.
Steffensen, J.P., 1997. The size distribution of microparticles from selected segments of the Greenland Ice Core Project ice core representing different climatic periods. J. Geophys. Res. 102, 26755–26763.
Sugden, D.E., McCulloch, R.D., Bory, A.J.-M., Hein, A.S., 2009. Influence of Patagonian glaciers on Antarctic dust deposition during the last glacial period. Nat. Geosci. 2, 281–285.
Suggate, R.P., 1963. The fan surfaces of the central Canterbury Plain. N. Z. J. Geol. Geophys. 6, 281–287.
Swart, N., Fyfe, J.C., 2012. Observed and simulated changes in the Southern Hemisphere surface westerly wind-stress. Geophys. Res. Lett. 39.
Taylor, S.R. and McLennan, S.M. (1985) The Continental Crust: its Composition and Evolution.
Tippett, J.M., Kamp, P.J.J., 1993. Fission track analysis of the Late Cenozoic vertical kinematics of continental Pacific crust, South Island, New Zealand. J. Geophys. Res. 98, 16119–16148.
Vallelonga, P., Barbante, C., Cozzi, G., Gaspari, V., Candelone, J.-P., Van De Velde, K., Morgan, V.I., Rosman, K.J., Boutron, C.F., Cescon, P., 2004. Elemental indicators of natural and anthropogenic aerosol inputs to Law Dome, Antarctica. Ann. Glaciol. 39, 169–174.
Vallelonga, P., Gabrielli, P., Balliana, E., Wegner, A., Delmonte, B., Turetta, C., Burton, G., Vanhaecke, F., Rosman, K.J.R., Hong, S., Boutron, C.F., Cescon, P., Barbante, C., 2010. Lead isotopic compositions in the EPICA Dome C ice core and southern Hemisphere potential source areas. Quat. Sci. Rev. 29, 247–255.
Vallelonga, P., Gabrielli, P., Rosman, K., Barbante, C., Boutron, C., 2005. A 220 kyr record of Pb isotopes at Dome C Antarctica from analyses of the EPICA ice core. Geophys. Res. Lett. 32.
Wegner, A., Gabrielli, P., Wilhelms-Dick, D., Ruth, U., Kriews, M., De Deckker, P., Barbante, C., Cozzi, G., Delmonte, B., Fischer, H., 2012. Change in dust variability in the Atlantic sector of Antarctica at the end of the last deglaciation. Clim. Past 8, 135–147.
Wengler, M., Lamy, F., Struve, T., Borunda, A., Boening, P., Geibert, W., Kuhn, G., Pahnke, K., Roberts, J., Tiedemann, R., 2019. A geochemical approach to reconstruct modern dust fluxes and sources to the South Pacific. Geochem. Cosmochim. Acta 264, 205–223.
Winton, V., Dunbar, G., Bertler, N., Millet, M.A., Delmonte, B., Atkins, C., Chewings, J., Andersson, P., 2014. The contribution of aeolian sand and dust to iron fertilization of phytoplankton blooms in southwestern Ross Sea, Antarctica. Global Biogeochem. Cycles 28, 423–436.
Winton, V.H.L., Edwards, R., Delmonte, B., Ellis, A., Andersson, P.S., Bowie, A.R., Bertler, N.A.N., Neff, P., Tuohy, A., 2016. Multiple sources of soluble atmospheric iron to Antarctic waters. Global Biogeochem. Cycles 30, 421–437.